İSTANBUL TECHNICAL UNIVERSITY ★ INSTITUTE OF SCIENCE AND TECHNOLOGY

COMPLIANT MECHANISM CASE STUDIES AND DYNAMICAL ANALYSIS OF A ROTATIONAL COMPLIANT DOUBLE DWELL MECHANISM

M.Sc. Thesis by
Barboros BENSOY

Department : Mechatronic Engineering

Programme : Mechatronic Engineering

JUNE 2009

İSTANBUL TECHNICAL UNIVERSITY ★ INSTITUTE OF SCIENCE AND TECHNOLOGY

COMPLIANT MECHANISM CASE STUDIES AND DYNAMICAL ANALYSIS OF A ROTATIONAL COMLIANT DOUBLE EXACT DWELL MECHANISM

M.Sc. Thesis by
Barbaros Bensoy
(518061002)

Date of submission : 04 May 2009
Date of defence examination: 05 June 2009

Supervisor (Chairman) : Assis. Prof. Dr. Ümit SÖNMEZ (ITU)
Members of the Examining Committee : Assis. Prof. Dr. M. Salih DOKUZ (ITU)
Assis. Prof. Dr. Erdinç ALTUĞ (ITU)

JUNE 2009

İSTANBUL TEKNİK ÜNİVERSİTESİ ★ FEN BİLİMLERİ ENSTİTÜSÜ

ESNEK MEKANIZMA ÇALIŞMALARI VE ROTASYONEL İKİLİ TAM BEKLEME ESNEK MEKANIZMASININ DİNAMİK ANALİZİ

YÜKSEK LİSANS TEZİ
Barboros BENSOY
(518061002)

Tezin Enstitüye Verildiği Tarih : 04 Mayıs 2009
Tezin Savunulduğu Tarih : 05 Haziran 2009

Tez Danışmanı : Yrd. Doç. Dr. Ümit SÖNMEZ (İTÜ)
Diğer Jüri Üyeleri : Yrd. Doç. Dr. M. Salih DOKUZ (İTÜ)
Yrd. Doç. Dr. Erdinç ALTUĞ (İTÜ)

HAZİRAN 2009

FOREWORD

I would like to express my thanks to my supervisor Ass. Prof. Ümit Sönmez to let me to study such a multidiciplinary subject that help my ability in such a design process improve regardless of the dificulties encountered during the thesis stage.

Finally, for giving infinite support and patience, I would like to thank my family and friends.

May 2009

Barboros Bensoy

Mechatronic Engineer

TABLE OF CONTENTS

Page

ABBREVIATIONS

MEMS : Micro electro mechanical systems
FEM : Finite element method
CCAR : Compliant contact-aided revolute
LPCVD : Low pressure chemical vapor deposition
PRBM : Puseido rigid body model

LIST OF FIGURES

Page

COMPLIANT MECHANISM CASE STUDIES AND DYNAMICAL ANALYSIS OF A ROTATIONAL COMPLIANT DOUBLE EXACT DWELL MECHANISM

SUMMARY

Complinat mechanisms have a wide range of usage in our daily life. This brings a lot of advantages of compliant mechanisms to the applications. In the last decade, as the manufacturing techniques had quick progress in macro and nano dimensions. As the manufacturing is miniaturized compliant mechanisms are design to be MEMS. This brings the advantages of MEMS: Less space, low cost, production in one place and no need to assembly. Because MEMS applications are spreading parallel to the studies in mechanism design, the methodology and solution procedures have been focused deeply. These subjects are handles in literature generally in three groups: Theoritical solutions, designing by the help of FEM and optimization and lastly manufacturing in real dimensions. As it is not possible to manufacture in micro level in most cases, making of the mechanism in macro level gives a lot of information about the design. Compliant mechanisms displacement range makes the theoretical solutions of kinematic analysis difficult. So, non-linear theory with numerical methods are implied. As the theoritical solution methods are not practical in some cases, FEM is used. In this research, a linear compliant dwell mechanism's analysis and sythesis methods are investigated and the results are reported. By using ANSYS FEM program bending and buckling of initially straight beams and the forve-deformation charactheristic of a bistable mechanism example is solved. This studies can be compiled under the title of compliant mechanism studies which helped to understand the methodology of analysis and sythesis of these mechanisms. A rotational comliant exact dwell mechanism where a non-continous motion is taken from a continous motion is dynamically analysed. The mechanism is build in macro level to validate the results.

ESNEK MEKANIZMA DURUM ÇALIŞMALARI VE ROTASYONEL İKİLİ TAM BEKLEME ESNEK MEKANIZMASININ DİNAMİK ANALİZİ

ÖZET

Esnek mekanizmalar günlük yaşantımızda birçok alanda avantajlar sağlamaktadır. Son yıllarda, imalat yöntemlerinin mikro ve nano düzeylere indirgenebilmesiyle esnek mekanizmalar MEMS olarak da üretilip, bunların daha az alanda ve maliyetle, montaj yapılmaksınız, tek bir düzlemde imal edilebilmeleri mümkün kılınmıştır. MEMS uygulama alanlarının esnek mekanizma tasarım alanındaki gelişmelerden beslenmesi nedeniyle, bu tasarım üzerine metodoloji ve çözüm yöntemleri türetildiği bir çalışma alanı oluşmuştur. Bu tür çalışmalar literatürde genellikle üç gruba ayrıldığı görülür: Teorik çözümle tasarım yöntemi, FEM paket programların kullanılarak tasarımın belirlenmesi veya mekanizmanın gerçek boyutlarında imal edilmesi. İmalatın gerçek boyutlarda mümkün olmadığı çalışmalarda makro düzeyde imalat tasarımın doğrulanması açısından önemlidir. Esnek mekanizmaların hareket kabiliyeti kinematik analizleri oldukça zorlaştırmış, doğrusal olmayan iteratif çözüm yöntemlerinin kullanılmasını zorunlu kılmıştır. Bu çalışmada literatürde sıkça karşılaşılan esnek bekleme mekanizmalarının doğrusal hareket çıkışı olan bir çeşidinin analiz ve sentez yöntemleri incelenmiş, sonuçları sunulmuştur. FEM paket programı olan ANSYS kullanılarak eğilme ve burkulma analizleri yapılmış, örnek olarak verilen bir bistable esnek mekanizmanın kuvvet-deformasyon eğrisi elde edilmiştir. Tüm bu çalışmalar esnek mekanizma çalışmaları başlığı altında toplanıp çözüm metodlarının kavranmasında yardımcı olmuştur. Uygulamada arzu edilen, sürekli bir hareket ile süreksiz bir çıkışın elde edildiği rotasyonal esnek bekleme mekanizmasının dinamik davranışı analiz edilmiştir. Mekanizma büyük ölçeklerde imal edilerek tasarım doğrulaması yapılmıştır.

1. INTRODUCTION

1.1 Definition of the Compliant Mechanisms

A compliant mechanism is called fully or partially compliant depending on the existing of traditional links and joints. A fully compliant mechanism does not require assembly of its parts. The mechanism investigated in this research is a partially compliant mechanism.

1.2 Advantages of Compliant Mechanisms

Compliant mechanisms may be considered for use in a particular application for a variety of reasons. The advantages of compliant mechanisms may be considered in two categories: cost reduction (part-count reduction, reduced assembly time and simplified manufacturing processes) and increased performance (increased precision, increased reliability, reduced wear, reduced weight and reduced maintenance) [1]. An advantage of compliant mechanisms is the potential for a dramatic reduction in the total number of parts required to accomplish a specified task. Some mechanisms may be manufactured from an injection-moldable material and be constructed of one piece. For example, consider the compliant overrunning clutch shown in figure 1.1 (a) and its rigid-body counterpart shown in figure 1.1(b). Considerably fewer components are required for the compliant mechanism than for the rigid mechanism. The reduction in part count may reduce manufacturing and assembly time and cost. The compliant crimping mechanism and its rigid-body counterpart illustrated in figure 1.2 are other examples of part reduction.

Compliant mechanisms also have fewer movable joints, such as pin (turning) and sliding joints. This results in reduced wear and need for lubrication [1]. These are valuable characteristics for applications in which the mechanism is not easily accessible, or for operation in harsh environments that may adversely affect joints.Reducing the number of joints can also increase mechanism precision, because

backlash may be reduced or eliminated. This has been a factor in the design of high-precision instrumentation.

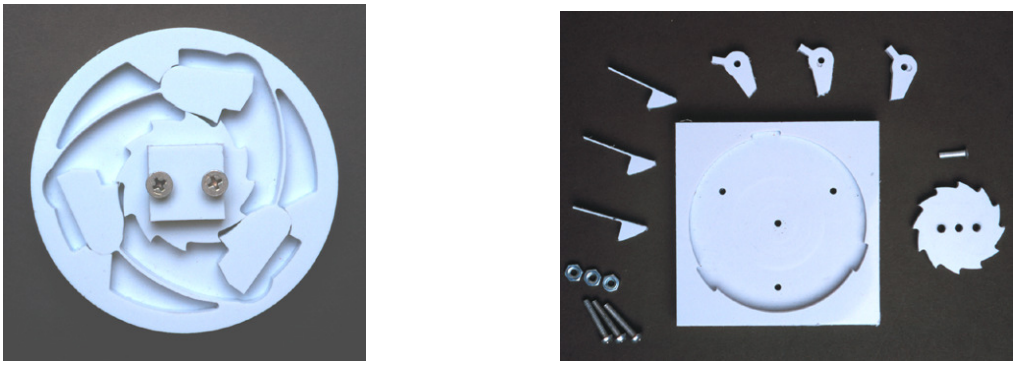

(a) (b)

Figure 1.1: (a) Compliant overrunning clutch and (b) its rigid-body counter-part dissassembled

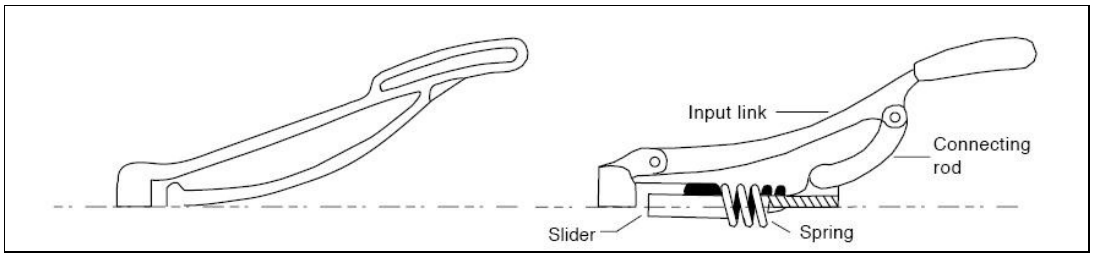

(a) (b)

Figure 1.2: (a) Compliant crimping mechanism developed by AMP Inc., and (b) its rigidbody counterpart

An example of a compliant mechanism designed for harsh environments is shown in figure 1.3. This simple gripping device holds a die (such as a computer chip) during processing. The die must be transported between several different chemicals without becoming damaged. Made of Teflon (inert to the chemicals in which it is placed) the gripper holds the die without external force. Because compliant mechanisms rely on the deflection of flexible members, energy is stored in the form of strain energy in the flexible members. This stored energy is similar to the strain energy in a deflected spring, and the effects of springs may be integrated into a compliant mechanism's design. In this manner, energy can easily be stored or transformed, to be released at a later time or in a different manner. A bow-and-arrow system is a simple example. Energy is stored in the limbs as the archer draws the bow; strain energy is then transformed to the kinetic energy of the arrow.

Figure 1.3: Compliant die grippers used to hold a die during process in several different harsh chemicals

These energy storage characteristics may also be used to design mechanisms that have specific force–deflection properties, or to cause a mechanism to tend to particular positions. For example, we can consider a robot end effector that was designed to have a constant output force regardless of the input displacement. It is possible to realize a significant reduction in weight by using compliant mechanisms rather than their rigid-body counterparts. This may be a significant factor in aerospace and other applications. Compliant mechanisms have also benefited companies by reducing the weight and shipping costs of consumer products.

Another advantage of compliant mechanisms is the ease with which they are miniaturized. Simple microstructures, actuators, and sensors are seeing wide usage, and many other MEMS show great promise. The reduction in the total number of parts and joints offered by compliant mechanisms is a significant advantage in the fabrication of micromechanisms. Compliant micromechanisms may be fabricated using technology and materials similar to those used in the fabrication of integrated circuits.

1.3 Disadvantages of Compliant Mechanisms

Although offering a number of advantages, compliant mechanisms present several challenges and disadvantages in some applications. Perhaps the largest challenge is the relative difficulty in analyzing and designing compliant mechanisms. Knowledge of mechanism analysis and synthesis methods and the deflection of flexible members is required. The combination of the two bodies of knowledge in compliant

mechanisms requires not only an understanding of both, but also an understanding of their interactions in a complex situation. Since many of the flexible members undergo large deflections, linearized beam equations are no longer valid. Nonlinear equations that account for the geometric nonlinearities caused by large deflections must be used. Because of these difficulties, many compliant mechanisms in the past were designed by trial and error. Such methods apply only to very simple systems that perform relatively simple tasks and are often not cost-efficient for many potential applications. Theory has been developed to simplify the analysis and design of compliant mechanisms, and the limitations are not as great as they once were. Even considering these advances, however, analysis and design of compliant mechanisms are typically more difficult than for rigid-body mechanisms. Energy stored in flexible elements has been discussed as an advantage, since it can be used to simplify mechanisms that incorporate springs, obtain specified force–deflection relationships, and store energy that is transferred or transformed by the mechanism. However, in some applications, having energy stored in flexible members is a disadvantage. For example, if a mechanism's function is to transfer energy from the input to an output, not all of the energy is transferred, but some is stored in the mechanism. Fatigue analysis is typically a more vital issue for compliant mechanisms than for their rigid-body counterparts.

Since compliant members are often loaded cyclically when a compliant mechanism is used, it is important to design those members so they have sufficient fatigue life to perform their prescribed functions.

The motion from the deflection of compliant links is also limited by the strength of the deflecting members. Furthermore, a compliant link cannot produce a continuous rotational motion such as is possible with a pin joint.

2. BACKGROUND

2.1 Literature Review of Large Deflection Analysis of Flexible Beams Using Elastica Theory

Compliant mechanisms usually undergo large deflection of its flexible links. Large deflection introduces geometric nonlinearities in the mechanism model. Classical formulation of large deflection analyses was initiated by Jacob Bernoulli who showed that beam curvature at any point is proportional to the bending moment at that point. Euler obtained several solutions of Elastica problems [2]. When deflections become large, beam curvature can no longer be approximated. The governing differential equations are expressed in terms of nonlinear functions that are typical of flexible straight beams, generally leading to highly implicit relationships involving elliptic integrals and functions.

The force deflection of an end loaded cantilever beam considering large deflections are investigated using elliptic integrals by Bisshopp and Drucker [3]. This investigation is frequently used in nonlinear finite element codes as a benchmark test case. Frisch-Fay had written a book on nonlinear bending and deflections of beam in order to fill the gap in nonlinear problems in the static of thin rods [4]. The undulating Elastica, the flexible beam with point of inflections along the beam, was formulated by Shoup and McLarnan [5]. They [6] also presented nonlinear equations of fixed-fixed Elastica. The fixed-fixed flexible strip non-dimensional load vs. deflections and bending moment vs. deflection curves were presented by Shoup [7]. The fixed-fixed flexible strip having one end constrained in a slider has the advantage of deflecting in the direction of the applied load. Gorski presented a review based on finite elastic deflection of beams taking into consideration more than two hundreds published works [8]. He emphasized particularly on the exact solutions of the Bernoulli-Euler equation. Mattiasson studied exact solution of some large deflection of beam and frame problems [9]. Naveee and Elling investigated the equilibrium configurations of a flexible cantilever beam subjected to end load with an inclination [10]. The compliant mechanism now presented uses a buckling elastic

element to create a dwell motion. Rigid finite dwell linkages are consist of at least 6-8 links. The proposed compliant mechanisms is a five-bar mechanisms and may be designed for less number of links by fabricating the follower, the slider and coupler spring from one piece.

2.2 MEMS

Micro-electro-mechanical systems (MEMS) provide a way to integrate electrical and computer circuitry with mechanical sensors or other mechanical elements. Therefore, they promise savings in cost, space, and manufacturing time for many applications.

2.2.1 Fabrication

This process, called surface micromachining, is the method most similar to conventional integrated circuit processing. Surface micromachining takes place on a silicon wafer using techniques similar to those used for integrated circuit manufacturing. In this section, the fabrication of a beam which is fixed on both ends is demonstrated to illustrate the process. Such a beam might be used to test for residual compressive stress by observing the buckling of the beam. The beam's typical size would be about fifty to one hundred microns long.In the first step, a thin layer of silicon oxide is deposited over the silicon substrate using low pressure chemical vapor deposition (LPCVD). This oxide layer is then patterned using a process known as planar lithography. The oxide is etched away in areas where the mechanical structures will be anchored to the substrate, as shown in figure 2.14. the oxide using hydroflouric acid. The completed beam is shown in figure 2.15. A second or even third layer of oxide and polysilicon may also be added to produce more complex structures. In this way, mechanical motors, mechanisms, and several different types of actuators have been produced. Several problems remain to be overcome in surface micromachining. One of the most serious is called "stiction." While drying after the release etch, capillary action in the evaporating liquid can pull free structures down, causing them to contact the substrate. Some force, possibly Van der Waals forces, causes the structures to remain stuck to the substrate even after drying is completed. The structures will then move only after a large force is applied to them. A similar thing happens any time a structure touches the substrate. Work is continuing to find ways to solve this problem [11]. The material involved represents

another limitation to surface micromachining. Polysilicon is a very high-strength material, with an ultimate strength of about $1.2*10^4$ bar [11]. However, it is also a very brittle material, with almost no yielding before fracture. It also has a Young's modulus of about $2*10^4\ N/mm^2$. These properties make it almost as stiff as steel, with about the same ultimate strength as a high-strength, brittle steel. However, if deflections are desired, as in compliant mechanisms, it tends to fail catastrophically if its strength is exceeded. This means that compliant mechanisms must be carefully designed to keep stress well under the strength. Another problem inherent with surface micromachining is the use of more than one layer of polysilicon.

More layers allow more complexity in the design; however, they also add cost and complexity to the manufacturing process, particularly if the extra layers are to be flat. If extra layers are simply deposited over lower layers, they will keep all of the topology of the underlying layers. While this fact is beneficial for some elements, it can be detrimental for others. While the layers can be planarized using a process known as chemomechanical polishing, this extra step is costly and allows more room for processing errors. Because of the problems inherent with multiple layers, surface micromachining is often limited to two non-planar layers. While two layers are enough to create grounded pin or prismatic joints, floating joints are much more difficult to make. For this reason, compliant mechanisms form a vital part of many MEMS devices. Because they gain motion by bending, compliant mechanisms often can be produced using only one layer of polysilicon, allowing considerable savings in manufacturing cost.

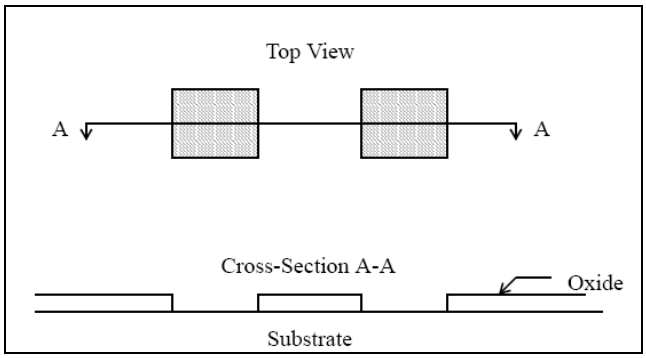

Figure 2.1: An early step in the surface micromachining process. The oxide has been patterned to allow a mechanical structure to be anchored to the substrate

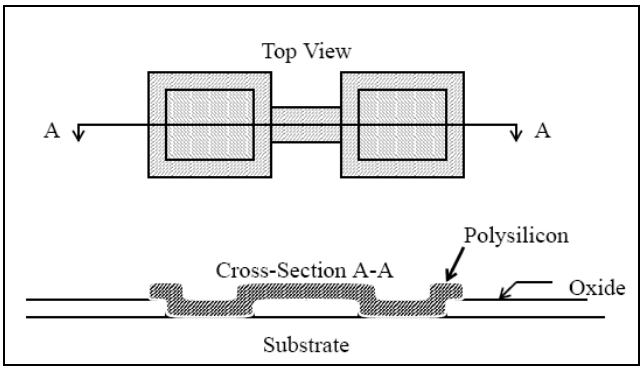

Figure 2.2: The fixed-fixed beam has now been patterned out of polysilicon

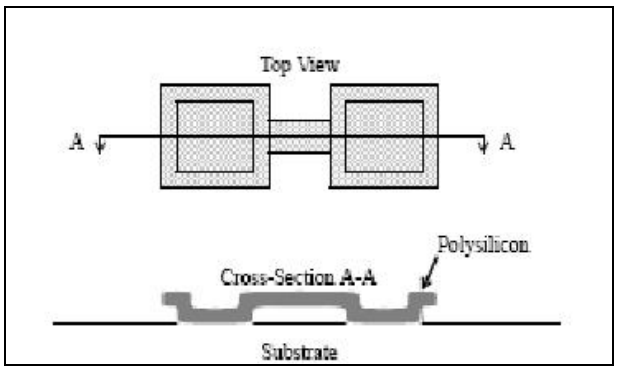

Figure 2.3: The completed fixed-fixed beam. The oxide under the beam has been removed by the release etch.

2.2.2 An example of compliant bistable mechanism

Bistable mechanisms are also compliant mechanisms due to its flexible members. They are used as switches and mechanical overload controls. A bistable mechanical device was designed using a single flexible strip to eliminate the toggle arm, spring, and stop in a conventional overcentering toggle mechanism [12]. Bistable mechanisms have two local minima of its total strain energy indicating the occurrence of two stable static equilibrium positions within its range of motion. This is similar to a commonly given example, the stability of a ball on a curved surface, as shown in Fig. 1. External force is required only between these two positions [12]. Microbistable compliant mechanisms are used effectively in microelectromechanical system (MEMS) design, such as microswitches, microvalves, and relays, since power consumption and heat dissipation are major concerns at microlevel [13].

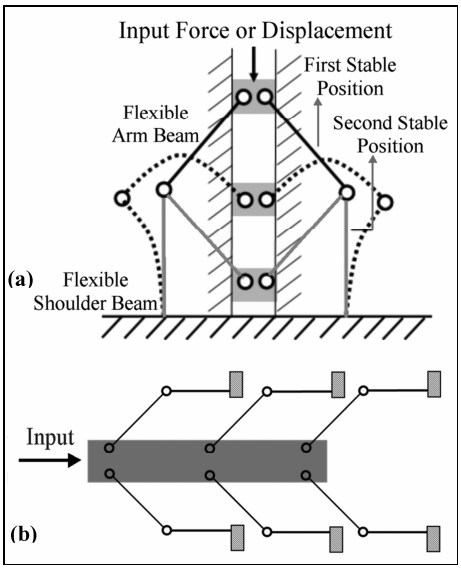

Figure 2.4: (a) Proposed compliant bistable mechanism design (b) The same design with several shoulder and arm beams which does not require a track to follow

The mechanism works as follows: As the slider moves, the flexible arm beams stay straight and push the flexible shoulder beams to sideways. The flexible arm beams behave as the rigid bodies until the critical buckling loads are reached. The buckling of arm beams might not be achieved and be explored (depending on cross sectional moment of inertia) in some of designs [14]. Until this instant, only the elastic shoulder beams deflect. After the critical buckling loads of the arm beams are reached, the beams buckle and continue to deflect until the snap-through buckling load (maximum applied load) of the bistable mechanism is reached [14]. Then, if a load controlled actuation is present, the slider snaps to the other stable position. While the slider snaps to a new stable position, the load on the flexible arm beams drops below the buckling load; then, the arm beams snap back to their rigid straight positions and their displacements become zero. When the slider reaches the second stable position, the flexible shoulder beams return to their original undeflected shapes. In this mechanism example study, a design method of this particular compliant bistable mechanism is used, and relative stiffness of the flexible beams is explored for several design parameters. A suitable candidate mechanism is selected using design tables and the quasistatic simulation of a selected compliant mechanism response is investigated [15].

The compliant bistable mechanisms usually employ large deflection of flexible members. Modeling of these mechanisms incorporates a broad range of knowledge in several areas, including kinematics, compliant mechanisms, bistable mechanisms, and nonlinear analysis of flexible beams. At the microscale, joint clearances can have a large effect on the force-displacement behavior of this type of mechanism. The sensitivity of the joint clearances and friction are kept out of the scope of the example.

Elastica Beam theory is used. Large deflection equations of the flexible beam is written in normalized form [14]. The equations are given briefly in the tırth chapter. The equations are solved numerically to obtain the nonlinear load deflection characteristics of a pin-pin beam subjected. The forces acting on a simple pinned-pinned segment are collinear along the line between the two pin joints. Moreover, the deflections of the flexible pinnedpinned segment are along this line. Pin ends do not carry moments; therefore, a pinned-pinned flexible beam is a two-force member. These observations will lead to model the pin-pin segment using a nonlinear spring expressed with a polynomial load deflection formula [15].

The cantilever beam shown in figure 2.5 can be represented as a PRBM, which is used for simplifying the nonlinear deflection analysis of the flexible beam members The cantilever beam shown in figure 2.5 can be represented as a PRBM, which is used for simplifying the nonlinear deflection analysis of the flexible beam members of compliant mechanisms with the aid of well-known rigid-body mechanism theory. The PRBM is composed of two parts: a rigid-body mechanism following the same trajectory with the tip of the original flexible beam and a nonlinear spring, which yields the same amount of angular deflection. The PRBM provides both the accuracy approximately 99.5% of the exact solution and the reduction in solution time[6]. The latter advantage can be especially important for optimization analyses and real-time control applications (e.g., MEMS). Three piecewise polynomials were specified by Howell for a range of n values. Instead of using three piecewise functions, a continuous rational function is fitted here to obtain the equivalent torsional spring constant to load deflection curve with a change in notation. It is considered here that the applied end force is composed of a vertical force component with the magnitude

P along the positive y axis and a horizontal force component with the magnitude $n\,P$ along the positive x axis.

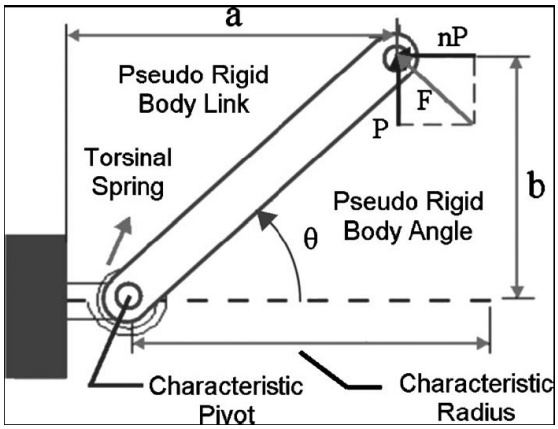

Figure 2.5: PRBM of a fixed-free beam

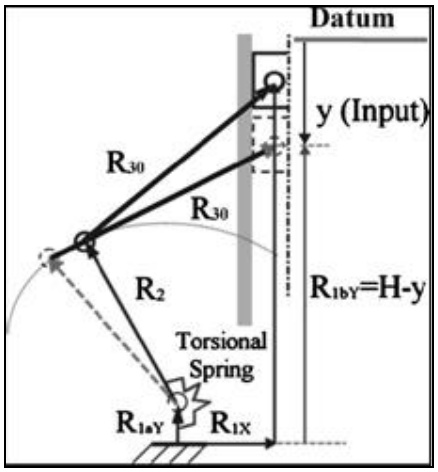

Figure 2.6: Representation of the half model before buckling

A new compliant bistable mechanism is proposed, which is composed of two flexible beams and a slider, as shown in figure 2.6. the corresponding reduced symmetric model including the closed loop vectors and the kinematic representation of the same model before the arm beam buckles are shown in figure 2.6, respectively. Kinematic analysis of this mechanism is studied using vector loop closure, equilibrium equations of mechanism members, and numerically solving nonlinear algebraic equations with the aid of Newton–Raphson method.

In this model, the pseudo-rigid-body parameters are updated as the loading conditions change at each iteration step, thus providing a more accurate model than that of the fixed parameters. There are two cases to be determined in order to investigate the behavior of the bistable compliant mechanism, depending on if the flexible arm beam buckles or not under the applied force.

Choosing a candidate mechanism requires suitable mechanism selection criteria. The following objective functions might be considered:

• A desirable contact force. If the bistable mechanism is used as a microswitch, then a desirable contact force is needed at the vicinity of the second stable position. This requires the maximization of the switchback force at the contact displacement.

• Low actuation force. Minimization of the actuation force until the maximum applied load could be another criteria.

• A desirable range of motion between two stable positions. Normalized range of motion for the slider (normalized to longest flexible beam), 1.0 - 1.5, might be achieved with this mechanism.

• Unstable range of motion. A positive slope of the load deflection plot is the indication of the stability, whereas a negative slope of the same plot is the indication of the instability. This parameter may be represented by its ratio to the slider range.

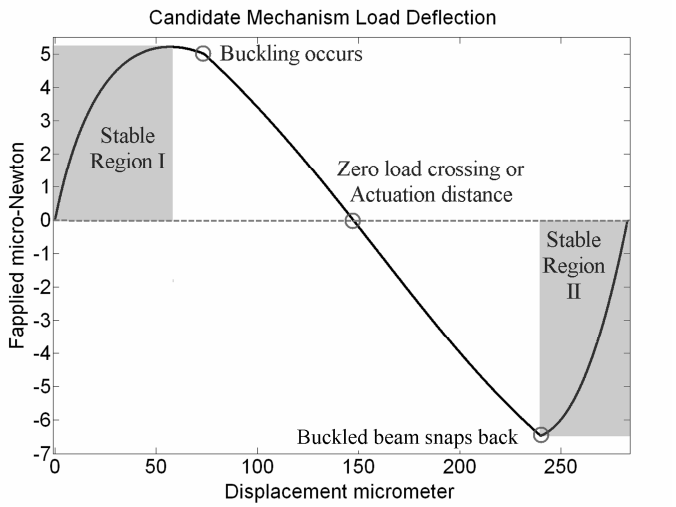

Figure 2.7: Load deflection plot of the candidate mechanism

2.3 Dwell Mechanisms

Most dwell mechanisms can be classified into two basic categories; finite dwell or momentary dwell. The difference between finite and momentary dwell is in the output motion duration. A finite dwell mechanism consists of a stationary output displacement operating region [16].

On the other hand a momentary dwell mechanism has a continuous nonlinear output motion function of input angle. In this case the first order time derivative of the output motion in the dwell region is instantaneously zero or approximately zero. Motion inaccuracies and approximations are sometimes acceptable for dwell applications.

A dwell motion can be described by four parameters: rise time, dwell time, return time, and rise also called lift as shown in figure 2.8 [17]. The dwell accuracy may be defined as the difference between the desired output position and the actual output position; and it equals to zero for an exact dwell. An exact dwell is very difficult to achieve even with optimal synthesis of 6-8 bar rigid linkages.

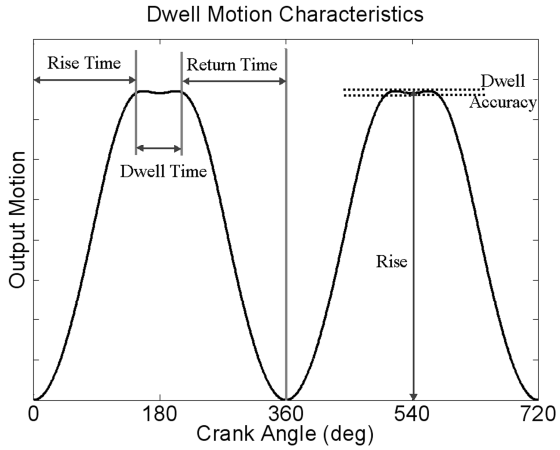

Figure 2.8: Dwell motion characteristics

Linkage type dwell mechanisms are comparatively less expensive to manufacture than cams and other intermittent motion mechanisms. Dwell motion can be obtained by rigid linkages with the use of coupler curves having straight line or circular arc segment [18]. Designing a rigid dwell linkage; the usual approach is to find a four bar linkage with a suitable coupler curve having either straight or circular arc segment and adding the two more links to obtain a dwell linkage [18].

In compliant dwell mechanisms; rise time, return time, dwell time and lift characteristics depend on the force and displacement interaction between the coupler and the follower rather than displacement interaction as in regular rigid body mechanism.

2.3.1 Analysis and synthesis of a translational compliant dwell mechanisms

2.3.1.1 Kinematic analysis of the compliant dwell mechanism

A translational compliant dwell mechanism is shown in figure 2.9. The mechanism consists of a rigid crank, a linear draw-bar spring as a coupler and a slider attached to an initially straight flexible beam. Draw bar springs consist of two sliding wire frames squeezing a compression spring; therefore it is easy to manufacture them with the desired length and the stiffness.

The design objective of the compliant mechanism is to obtain dwell motion, using the buckling phenomena of the flexible beam. During the rotation, the crank pulls left end of the coupler causing the coupler spring to be compressed and the right end of it to pull the flexible beam. While the horizontal force component of the draw-bar coupler spring is below the critical buckling load of the flexible beam; the slider attached to the flexible beam does not move creating an exact first dwell. When the horizontal force reaches the critical buckling load of the flexible beam; it buckles, providing displacement to the slider. As the crank continues to rotate, a momentary second dwell occurs.

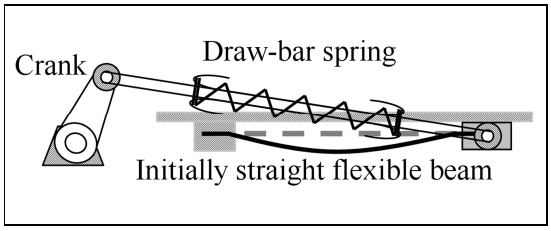

Figure 2.9: Members of the compliant long dwell mechanism

This investigation deals with the displacement analysis of the compliant dwell mechanism and presents a methodology to synthesize a compliant dwell mechanism for required dwell time, maximum rise and mechanism space requirements considering several mechanism design parameters. Dwell mechanism charts are obtained for a range of mechanism design parameters. The mechanism dimensions and coupler stiffness are chosen to obtain required dwell time and maximum rise from the design charts. Once the mechanism parameters are decided using the design charts; the method presented in this research provides a means to analytically calculate the position of the slider as the crank rotates quasi-statically through a complete cycle of 360°.

Kinematic analysis of this compliant dwell mechanism requires solution of a nonlinear equation set containing: loop closure equation; crank, linear spring and slider static equilibrium equations; large deflection polynomial of flexible buckling beam.

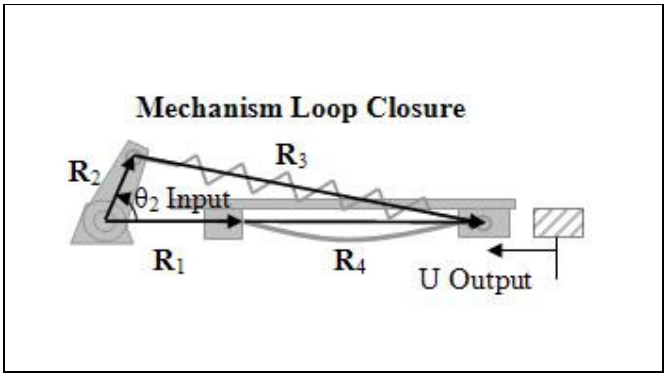

Figure 2.10: Loop closure of the compliant dwell mechanism

A closed vector loop for the compliant mechanism is shown in figure 2.10. Loop closure equation and its horizontal and vertical vector components yields:

$$\vec{R_2} + \vec{R_3} = \vec{R_1} + \vec{R_4} \quad \textbf{(2.1)}$$

$$R_2 \cos\theta_2 + R_3 \cos\theta_3 - R_4 = R_1 \quad \textbf{(2.2)}$$

$$R_2 \sin\theta_2 + R_3 \sin\theta_3 = 0 \quad \textbf{(2.3)}$$

The free body diagram of the compliant dwell mechanism and static equilibrium of mechanism parts are shown in figure 2.11.

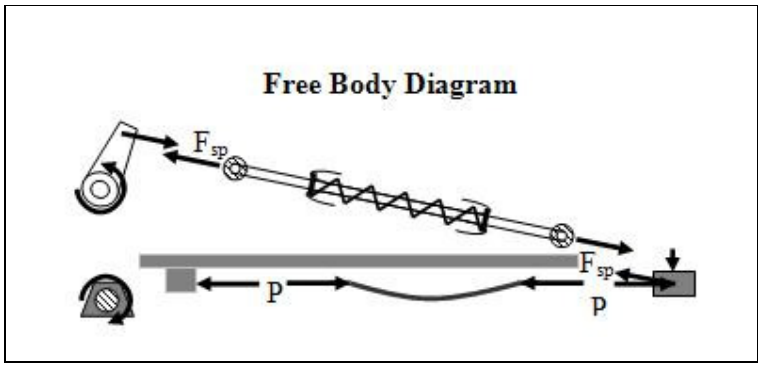

Figure 2.11: Free body diagram of compliant dwell mechanism

Moment equilibrium of the crank, and force equilibrium of the coupler spring and the slider may be expressed as:

$$T - F_{sp} \sin\theta_3 R_2 \cos\theta_2 + F_{sp} \cos\theta_3 R_2 \sin\theta_2 = 0 \quad \textbf{(2.4)}$$

$$F_{sp} = k_{sp}(R_3 - R_{30}) \quad \textbf{(2.5)}$$

$$F_{spring} \cos(\theta_3 - \pi) + P_{elastica} = 0 \quad \textbf{(2.6)}$$

Nonlinear large deflection formulas for a fixed-fixed flexible beam is expressed with a 4th order polynomial as follows:

$$P_{elastica} = A_4 U^4 + A_3 U^3 + A_2 U^2 + A_1 U + A_0 \quad \textbf{(2.7)}$$

Where A_n with $n = 0…4$, are described as follows,

$$A_n = (EI/L^{n+2}) a_n \quad \textbf{(2.8)}$$

In above Eq. (2.8) a_n $n = 0…4$, are the normalized load-deflection polynomial curve fit coefficients.

When a horizontal force applied to the flexible beam is less than the critical buckling load of the fixed-fixed flexible beam $P < (P_{cr} = 4*\pi^2*EI/L^2)$ the slider does not move and behaves like a ground link $R_4=L_{beam}$. In this case, simulation of the mechanism can be accomplished by solving Eqs. (2.2-2.5) for the unknowns T, F_{sp}, R_3, θ_3. As the crank rotates and the horizontal force component exceeds the critical buckling load, then the slider will move, creating the potential for a second dwell. Slider motion under this operating condition can be simulated by solving Eqs. (2.2-2.7) for the unknowns T, F_{sp}, R_3, θ_3, P, and $R_4 = L_{beam}-U$ as a function of crank angle θ_2.

2.3.1.2 Solution procedure

Two different sets of equations need to be solved corresponding to the buckled or unbuckled state of the flexible beam. The unbuckled state is represented by Eqs. (2.2-2.5) with $R_4 = L_{beam}$; making the slider to behave like a ground link. These equations can be solved analytically or numerically for R_3 and θ_3. Spring force and torque may be calculated by solving Eq. (2.6) and Eq. (2.5) in the given order.

The large deflection buckled state (nonlinear load deflection analysis) of the flexible beam is represented by a 4^{th} order polynomial. Therefore total system simulation requires the solution of Eqs. (2.2,2.3) and Eqs. (2.7,2.8,2.9) by means of a nonlinear equation solver routine. Newton-Raphson method with a good initial guess is used in order to simulate the compliant mechanism response.

As the crank rotates quasi-statically through the complete cycle of 360°, the solution for the previous step is used as the initial guess for the next iteration step. In the vicinity of the buckling load, the crank angle increment is refined in order to simulate the system of equations accurately to overcome the difficulty caused by the buckling of the flexible beam.

2.3.1.3 Synthesis methodology

A synthesis methodology is introduced in this section to determine the dimensions of the compliant mechanism and its flexible parts' stiffness parameters to obtain required rise height and dwell time under a space limitation constraint and an optional flexible beam force requirement.

As an example a compliant dwell mechanism with *1.2-1.25 cm* maximum rise, *170°-190°* dwell time, *20 cm*10 cm* mechanism space allowance and optional a *0.20-0.40N* maximum flexible beam force requirement is designed explaining each step along the way.

Buckling beam parameters: Beam's material, beam's length and cross sectional area dimensions have to be determined keeping the maximum bending stress below the elastic limit (yield strength) for the required rise. Assuming the beam length is inextensible after the buckling, the primary beam stresses are due the bending.

The buckled flexible beam's curvature changes as the flexible beam deflects. The bending stress must be kept below the bending yield stress, within the operating elastic range of the material. The bending moment along a fixed-fixed beam equation may be written as,

$$M = 2k\sqrt{EIP}\cos\varphi \qquad \textbf{(2.9)}$$

For a fixed-fixed flexible initially straight flexible beam with no offset *(H=0)*, maximum bending moment occurs at the each ends and in the middle of the beam. Primary bending stresses is expressed by the following formula,

$$\sigma_b = \frac{M}{I} y \tag{2.10}$$

Using Eqs. (2.9,2.10); the following maximum bending stress of the rectangular cross section area may be calculated as,

$$\sigma_{\max} = 2k\sqrt{\frac{3EP}{bt}} \tag{2.11}$$

Where b and t are cross sectional dimensions width, thickness and k is the shape factor respectively.

Flexible deflected beam shapes are also needed to comply with the mechanism space requirements and they might be calculated using formulas given in [14]; the reader should refer to the proposed investigation for their derivation [15].

$$\begin{aligned} x_{elastica} &= \pm(2a/d)\sqrt{2/d}\left[E(k,\varphi_2) - E(k,\varphi_1)\right] \mp (a/d)\sqrt{2/d}\left[F(k,\varphi_2) - F(k,\varphi_1)\right] \\ &\pm k(2b/d)\sqrt{2/d}\left[\cos\varphi_2 - \cos\varphi_1\right] \end{aligned} \tag{2.12}$$

$$\begin{aligned} y_{elastica} &= \pm(2b/d)\sqrt{2/d}\left[E(k,\varphi_2) - E(k,\varphi_1)\right] \mp (b/d)\sqrt{2/d}\left[F(k,\varphi_2) - F(k,\varphi_1)\right] \\ &\pm k(2a/d)\sqrt{2/d}\left[\cos\varphi_1 - \cos\varphi_2\right]. \end{aligned} \tag{2.13}$$

Where $x_{elastica}$ and $y_{elastica}$ are the compliant beam coordinates, $a = 2p$, $b=2q$ and $d = (a^2+b^2)^{0.5}$.

Deflected beam shapes are plotted in figure 2.13, by observing the flexible beam contours, it is instantly recognizable that curvature expression can not be reduced to its linear form d^2y/dx^2; therefore linear theories do not work designing compliant mechanism exploring flexible member's deflections to its outmost. Most of the compliant mechanism studies require large deflecting members which could only be calculated either using exact nonlinear elastic theories or geometrically nonlinear FEM codes. Therefore compliant mechanism research is an interdisciplinary area of applied mechanics and mechanism design.

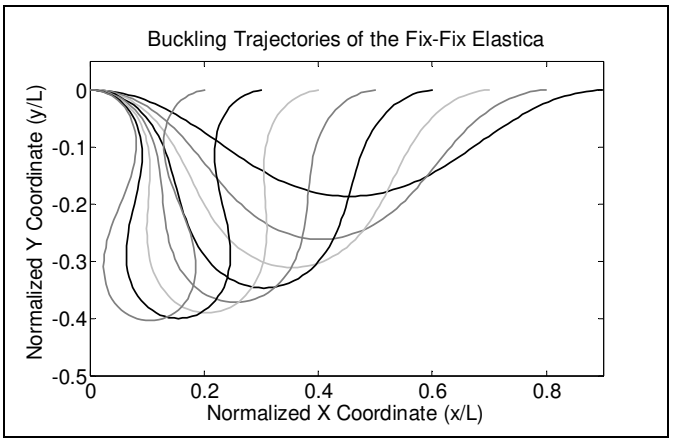

Figure 2.13: Large deflected shapes of fix-fix buckling beam

The beam maximum bending stress is independent of beam width. Increasing the beam width causes to increase the critical bucking load and the applied load for the required deflection $P = P\ (b,\ t^3)$, not the stresses $\sigma = \sigma\ (k,\ t^2)$. Therefore if the applied load requirement is considered, the optional case for the mechanism design, it could be adjusted to some extent by changing beam width resulting in the same stress.

Briefly the other remaining part of the synthesis consist of these steps: Choosing the lenght of the cranks, then picking the solution range from the design charts which are giving the dwell time and maximum rise, determining the spring stiffness coefficient and finally obtaining the mechanism response by the simulations.

2.3.1.4 Simulation results

Compliant dwell mechanism simulation results are presented in this section. There are two distinctive dwell areas: primary and secondary dwell. The primary dwell is an exact dwell and the secondary dwell is an instantaneous dwell. The secondary dwell takes place between crank angles *94°-267° (173°)*; so that during whole crank rotation cycle the mechanism dwells for *187°* which agree with the desired dwell time. This is a long exact dwell, taking approximately half of the full crank rotation angle. Horizontal component *P* of the linear spring load is shown in figure 2.16. The load increases first very rapidly until the flexible beam buckles. Until the buckling load is reached the flexible beam behaves as a rigid body and only the coupler spring deflects. After buckling, the horizontal force component stays fairly constant over the

secondary dwell region reaching *0.32 N* agreeing with the desired horizontal force requirement. A momentary dwell in this region has been tried to attain by keeping the horizontal force constant but failed. In this design; the secondary dwell is only instantaneous, because the small changes in horizontal forces cause considerable displacement of the flexible beam in the post buckling region. Figure 2.16 also demonstrates even though flexible beam force stays fairly constant after buckling it causes large deflections in the post buckling range.

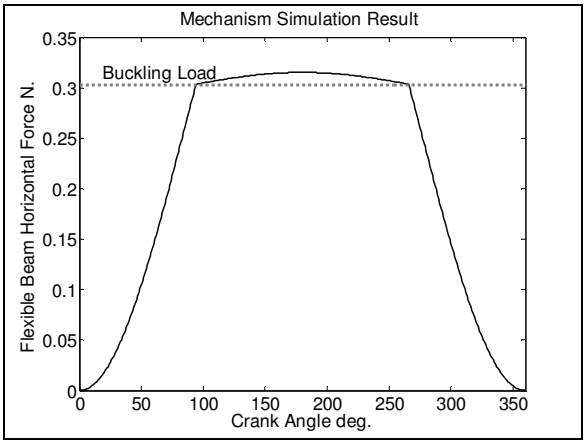

Figure 2.14: Flexible beam horizontal load versus crank angle

The coupler spring is compressed rapidly until the flexible beam buckles, after the buckling the coupler length stays fairly constant over the secondary dwell without reaching the draw-bar spring stopper.

Mechanism outlook is presented normalized to flexible follower length in Figure 16 for a range of *180˚* crank angle at every *60˚* crank angle increment. The fix-fix buckling beam shapes are also plotted in figure 2.16 using the nonlinear Elastica theory; demonstrating that the mechanism could fit to *20cm*10cm* space requirement.

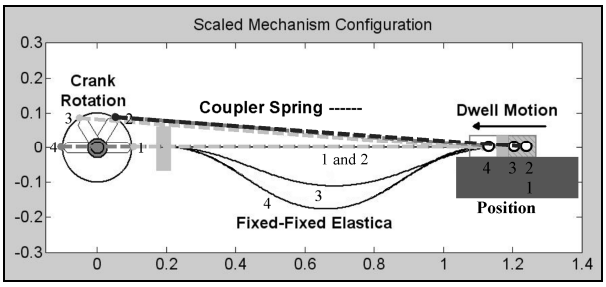

Figure 2.15: Mechanism's outlook as the crank rotates

2.3.2 Rotational exact dwell mechanism

Rotational dwell mechanisms are the mechanisms which takes a dwell motion from a continous rotational motion.

The mechanism works as follows: As the direct current motor starts its movement , it gives a constant velocity motion to the crank. The flexible arm beams are carefully to obtain the exact dwell motion by the help of the buckling phonomena. The distance between crank and the follower is approximately double of the beam that is between the follower and the ground. So that the first elastic beam buckles why the second beam is just compress in the postbuckling region. When the crank starts its movement, the long flexible arm beam forced to buckle and the short beam does not. This gives the first dwell region of the follower. As the crank moves the force applied to the follower by the long arm beam increases.

When the reaction force on the short beam reaches to the critical load the flexible arm beam buckles and moves to the second stable condition. As it reaches to the constant position the second dwell period starts. During this period the force on the tip of the long arm beam forces the second beam to elongate. As the crank moves the long beam becomes straight and forces the second beam to move to the first stable position so that the 360 degreee rotation of the crank has been completed.

As the mechanism is a bistable mechanism with an input of continous rotational motion the beams will buckle as expected in the design stage the dwell motion will occur. The other advantaga of the mechanism is that the response is not actuation varianted. The input of the system is the geomertic contsrains: crank, follower and beam element dimensions and where they linked to the ground.

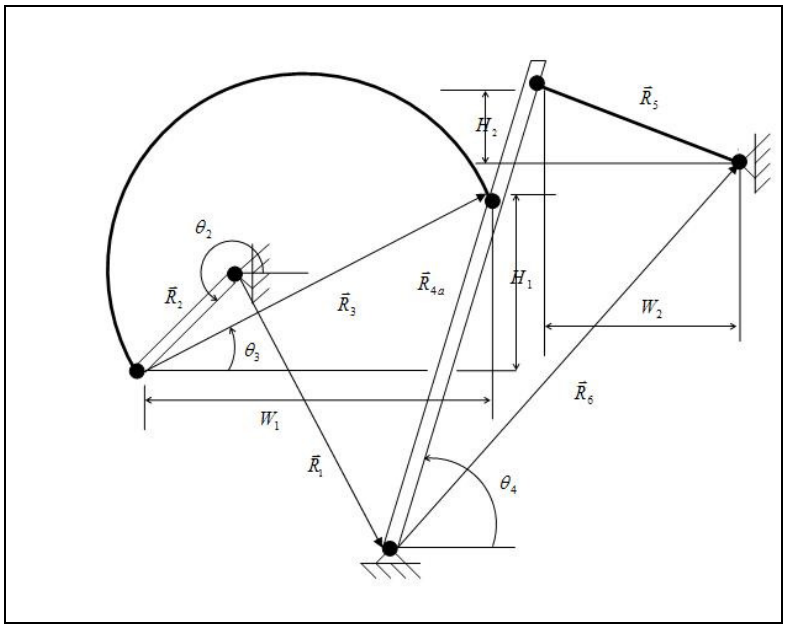

Figure 2.16: Geometric design parameters of the rotational exact dwell mechanism

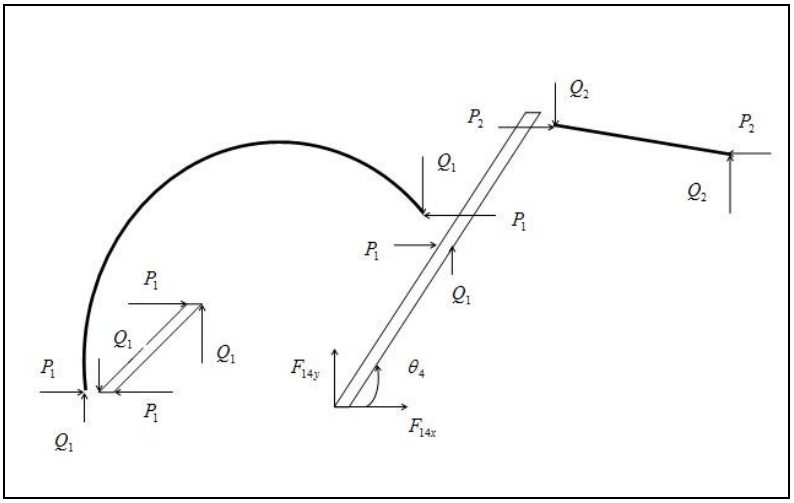

Figure 2.17: The Reaction forces on the follower, crank and flexible arm beam

3. COMPLIANT MECHANISM STUDIES USING FEM

3.1 Nonlinear Buckling Analysis

In this chapter non-linear buckling phonomena is focused under theoretical solutions and FEM analysis results.

3.1.1 Theoritical review of non-linear buckling of an initially straight beam

Consider the general flexible beam which is initially straight as shown in figure 3.1. The flexible beam is loaded by the applied vertical end force *Q*, horizontal end force *P*, and end moments M_1 and M_2.

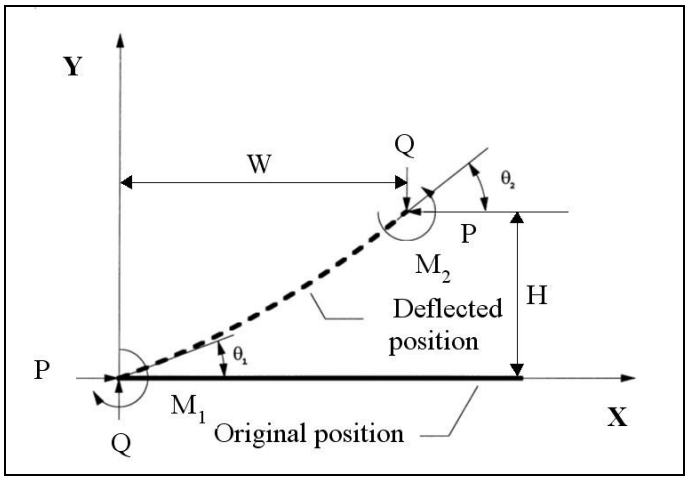

Figure 3.1: Beam segment under applied end loads and moments

The sign convention for *X* and *Y* is shown in figure 3.1. The summation of forces in the *X* direction and the summation of forces in the *Y* direction are equal to zero and the equilibrium conditions for these directions are satisfied. The product *EI* is the beam flexural rigidity and will be considered constant. The moment curvature relationship, the Bernoulli-Euler equation, can be written as,

$$\frac{d\Theta}{ds} = \frac{M}{EI}. \qquad \textbf{(3.1)}$$

Where $d\Theta/ds$ is the curvature, Θ is the beam angle measured from *X* axis, *s* is the length along the beam, and *M* is the internal bending moment. The moment equilibrium equation at a given point *(x, y)* can be expressed as;

$$M = -M_2 - Py + Qx. \tag{3.2}$$

Where M_2 is the applied moment at the right end of the beam, and *P* and *Q* are applied horizontal and vertical forces respectively as shown in figure 3.1. Substituting Eq. (3.2) into Eq. (3.1) and differentiating each side with respect to s gives,

$$EI\frac{d^2\Theta}{ds^2} = -P\frac{dy}{ds} + Q\frac{dx}{ds} \tag{3.3}$$

Substituting the expressions $dx/ds=\cos\Theta$ and $dy/ds=\sin\Theta$ into Eq. (3.3) results in,

$$EI\frac{d^2\Theta}{ds^2} = -P\sin\Theta + Q\cos\Theta \tag{3.4}$$

This equation is integrated as,

$$\frac{EI}{2}\left(\frac{d\Theta}{ds}\right)^2 = P\cos\Theta + Q\sin\Theta + C_0. \tag{3.5}$$

When Eq. (3.5) is solved for $d\Theta/ds$, it gives the following expression for the curvature.

$$\frac{d\Theta}{ds} = \pm\sqrt{\frac{2(P\cos\Theta + Q\sin\Theta + C_0)}{EI}}. \tag{3.6}$$

When the curvature is positive, the beam is concave up and when the curvature is negative the beam is concave down. The following equation can be obtained from Eq. 3.6.

$$ds = \pm d\Theta \Big/ \sqrt{\frac{2(P\cos\Theta + Q\sin\Theta + C_0)}{EI}}. \tag{3.7}$$

Using the following non-dimensional parameters;

$$w = \frac{W}{L} \quad h = \frac{H}{L} \quad p = \frac{PL^2}{EI} \quad q = \frac{QL^2}{EI} \quad m = \frac{ML}{EI} \quad c = \frac{C_0 L^2}{EI}. \tag{3.8}$$

Equation (3.7) becomes,

$$\frac{d\Theta}{ds} = \pm \frac{1}{L} \sqrt{2(p\cos\Theta + q\sin\Theta + c)}. \tag{3.9}$$

Equation (3.9) is integrated over the length of the beam to obtain

$$1 = \pm \int_{\Theta_1}^{\Theta_2} \frac{d\Theta}{\sqrt{2(p\cos + q\sin\Theta + c)}}. \tag{3.10}$$

The non-dimensional *x* coordinate of the flexible beam may be written as,

Similarly the non-dimensional *y* coordinate of the flexible beam is written as,

$$w = \pm \int_{\Theta_1}^{\Theta_2} \frac{\cos\Theta d\Theta}{\sqrt{2(p\cos + q\sin\Theta + c)}}. \tag{3.11}$$

Using Eqs. (1), (8) and (9) the following non-dimensional moment expression may be obtained.

$$m = \pm \int_{\Theta_1}^{\Theta_2} \sqrt{2(p\cos\Theta + q\sin\Theta + c)}\, d\Theta. \tag{3.13}$$

Using change of variables and integrals transforms as described in Elliptic Integrals Handbook by Byrd and Friedman [17], the above equations may be manipulated to obtain nonlinear algebraic equations containing elliptic integrals of first and the second kind. The complete derivations can be found in the referenced literature [15]. *F(k,φ)* and *E(k,φ)* are incomplete elliptic integrals of first and second kind respectively with modulus *k* and amplitude *φ*. If $\varphi = \pi/2$; these integrals are called complete elliptic integrals of first and second kind. These integrals might be defined as:

$$F(k,\varphi) = \int_0^{\varphi} \frac{1}{\left(1 - k^2 \sin^2\varphi\right)^{0.5}} d\varphi \tag{3.14}$$

$$E(k,\varphi) = \int_0^{\varphi} \left(1 - k^2 \sin^2\varphi\right)^{0.5} d\varphi \tag{3.15}$$

The complete normalized set of nonlinear equations for the initially straight flexible beam may be rewritten in the null form as,

$$-(p^2+q^2)^{0.25} \pm \left[F(k,\varphi_2) - F(k,\varphi_1)\right] = 0 \qquad \textbf{(3.16)}$$

$$-w(p^2+q^2)^{0.75} \pm p\left[2E(k,\varphi_2) - 2E(k,\varphi_1) - F(k,\varphi_2) + F(k,\varphi_1)\right] \pm 2qk(\cos\varphi_2 - \cos\varphi_1) = 0 \qquad \textbf{(3.17)}$$

$$-h(p^2+q^2)^{0.75} \pm q\left[2E(k,\varphi_2) - 2E(k,\varphi_1) - F(k,\varphi_2) + F(k,\varphi_1)\right] \mp 2pk(\cos\varphi_2 - \cos\varphi_1) = 0 \qquad \textbf{(3.18)}$$

The non-dimensional end moments result in,

$$p\cos\theta_1 + q\sin\theta_1 + (2k^2\sin^2\varphi_1 - 1)(p^2+q^2)^{0.5} = 0 \qquad \textbf{(3.21)}$$

$$p\cos\theta_2 + q\sin\theta_2 + (2k^2\sin^2\varphi_2 - 1)(p^2+q^2)^{0.5} = 0 \qquad \textbf{(3.22)}$$

Finally the flexible beam end angles θ_1 and θ_2 are related to elliptic integral amplitudes φ_1 and φ_2 by the following equations.

For a fixed-fixed beam with given end angles θ_1, θ_2 and the beam offset h; Eqs. (3.16, 3.17, 3.18, 3.21 and 3.22) might be solved for the unknowns; p, q, k, φ_1 and φ_2 while changing the normalized displacement $w=W/L$ as the input.

A nonlinear algebraic solution routine incorporating elliptic integral subroutines might be used to solve the equation set. Since these equations are highly non-linear they should not be directly included in mechanism simulation equations containing kinematic loop closure equations; they will increase the total number of equations and may cause convergence problems. Therefore load deflection characteristics of the fixed-fixed bucking beam must be represented by a suitable load deflection function (e.g. exponential, polynomial or rationales etc.)[18].

When a functional fit is used; the quality of the fit is measured by the correlation coefficient. However the correlation coefficient is the indication of the quality of the fit in a statistical sense and mostly provides a statistical point of view; but an accurate representation is needed in this research For example a polynomial fit of $\rho=0.9999$ is an accurate fit, whereas $\rho=0.9900$ is not for the simulation purposes. The correlation coefficient is represented by the following formula:

$$\rho = \left[1 - \sigma^2_{(y,x)} / \sigma^2_y\right]^{0.5}. \quad \textbf{(3.23)}$$

$$\sigma_y = \left[\sum_{i=1}^{N} (y_{exact} - y_{mean})^2 / (N-1)\right]^{0.5}. \quad \textbf{(3.24)}$$

Where y_{mean} is the mean value of the exact solution points and y_{exact} is the exact solution obtained using the nonlinear inextensible flexible beam deflection theory. In Eq. (23) $\sigma_{(y,x)}$ is defined as,

$$\sigma_{(y,x)} = \left[\sum_{i=1}^{N} (y_{exact} - y_{fit})^2 / (N-2)\right]^{0.5}. \quad \textbf{(3.25)}$$

Where y_{fit} represents the values approximated by the least squares polynomial fit and N is the number of discrete solution points.

The solution of the fixed-fixed beam with no offset $h=0$ and given end angles $\theta_1=0$, $\theta_2=0$ (geometric boundary conditions) are solved and presented in this section. The flexible beam does not deflect until a certain critical load is reached as shown in figure 3.2. The pre-buckling deformations of the fixed-fixed column are negligible; therefore the critical buckling load calculated by the linear theory (an eigen-value problem resulting in $4\pi^2$) is the same as the critical value obtained by the nonlinear theory.

Curve fitting to the normalized load deflection plot of fixed-fixed beam constraining the correlation coefficient to be $\rho > 0.9998$ has resulted in a 4th order polynomial with a correlation coefficient $\rho > 0.9999$. The polynomial is given by Eq. 3.26, and the corresponding fit to the exact solution is shown in figure 3.2.

$$p(u) = \frac{PL^2}{EI} = 29.27u^4 - 25.94u^3 + 25.86u^2 + 17.32u + 39.58 \quad \textbf{(3.26)}$$

The shape of the deflected beam with inflection points are determined by the shape of the undulating Elastica [11].

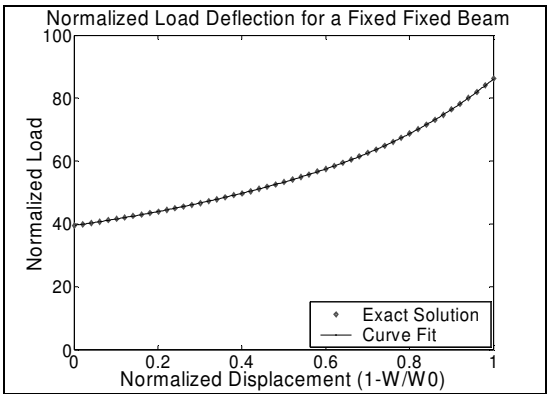

Figure 3.2: Buckling of the fixed-fixed beam; the exact Elastica solution and the corresponding 4th order fit

The only parameter that determines the shape is the modulus *k*, also called shape factor, in Eqs. (3.14-22) and it is used for calculating the maximum bending stresses of the buckled beam. A rational function is found to be more suitable to fit on the shape factor than the higher order polynomials. Curve fitting to the shape factor versus normalized deflection plot of fixed-fixed beam with constrain $\rho > 0.9998$ has resulted in a rational (2nd order/3rd order) with a correlation coefficient $\rho = 0.99988$. The exact solution of the shape factor and its corresponding fit is presented in figure 3.3, and it is given by the Eq. (3.27).

$$k = \frac{5910u^2 + 909u}{u^3 + 3789u^2 + 3627u + 73.84} \qquad \textbf{(3.27)}$$

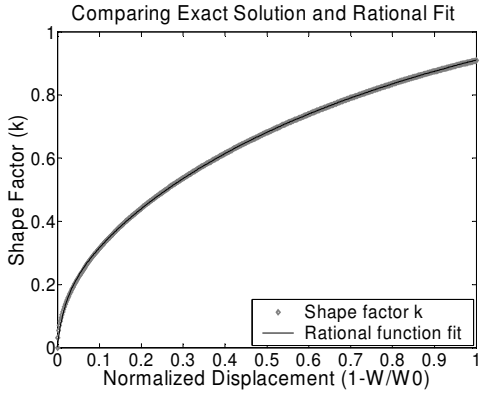

Figur 3.3: Fixed-fixed buckling beam shape factor k versus normalized deflection

3.1.2 Non-linear buckling analysis of an initially straight beam with ANSYS

In nature, mechanisms and materials give mostly non-linear respose which is difficult to model mathematically. To model these systems or parts of a system, there are commercial programs that solves the equations numerically. In these programs, there are mailny three steps to follow:

- Pre-processing
- Analysis
- Post-processing

In pre-processing step the model is prepared. The element type is chosen as BEAM188 as it is an element prepared specially for beams. Material of the beam is modeled as linear elastic. So, as the beam goes into the large deformation region, the beam doesn't have plastic deformation.

The analysis type is statical to perform a nonlinear deformation with force input in the specified range. Firstly, eigen buckling analysis has been done for the beam so that the critical force for the first mode of buckling is observed. In the non-linear analysis, the input force magnitude is chosen to be more than the critical force.

Loads are defined in the following step which are constraints and applied force. The displacement constraints were given on the joint to the ground on ux, uy, uz and my and mx so that the joint is modeled as a revolute joint connected to the ground. On the free end of the beam, the force is applied as on the –y direction. Allthough with this inputs the model will respond as it is applied only compressive stress and compressed by the force in the –y direction. As we consider the first mode of buckling shape, it is possible to initiate the buckling with an incrimental force on the midpoint of the beam on the x axis. As we apply 0.5 N on –y axis, 5*10e-3 N is applied on the x axis on the 51th node of the beam.

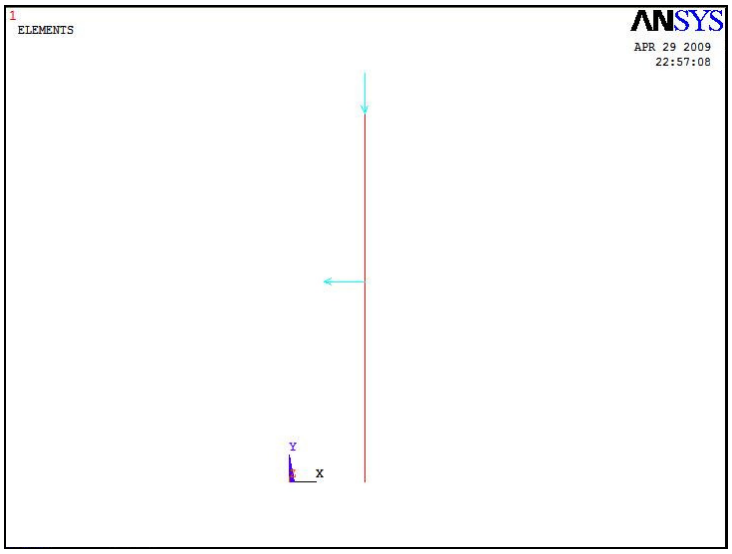

Figure 3.4: Forces applied on the free end and mid point of the beam element

In post-processing step the results are viewed. The deformed and undeformed shapes of the beam are viewed in the same window as in the figure 3.5.

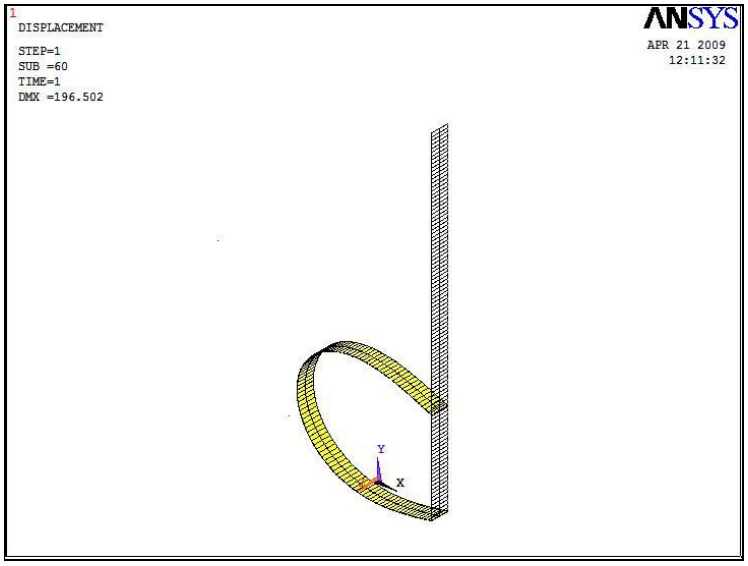

Figure 3.5: Deformed and undeformed shapes of the initially straight beam

Using the time history postpro menu in ANSYS, the force displacement results at each substep is listed and the graph of displacement of y axis to y component of the reaction forces are plotted as in the figure 3.6**.**

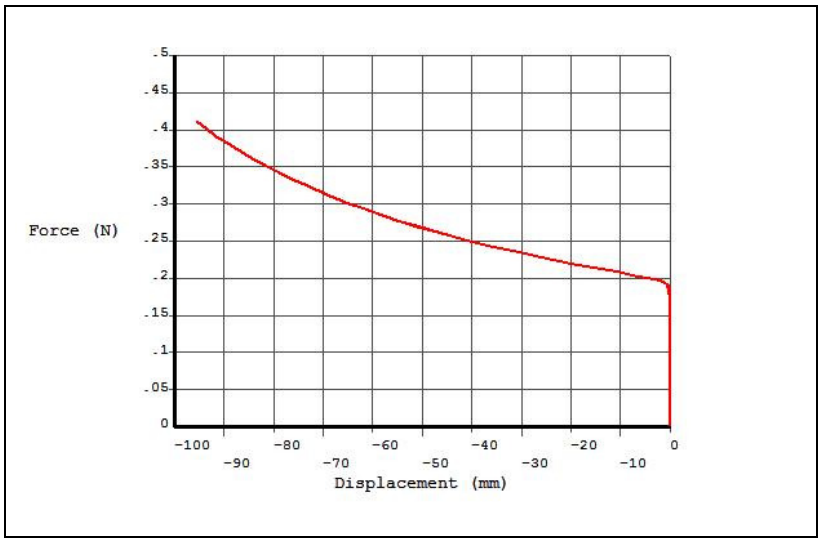

Figure 3.6: Load-deflection curve

In this solution, the critical load is approximated to Euler equation results. The euler equation for the pin-pin beam can be described as below.

$$P_c = \frac{E..I.\pi^2}{L^2} \tag{3.28}$$

$$P_c = 0.1985N$$

3.2 Force-Deflection Results of the Half Model of the Sample Bistable Mechanism

A parameter set including the shoulder beam: h_1=3.5 µm, w_1=2.0 µm, L_1=50 µm, and the arm beam: h_2=3.5 µm, w_2=10.0 µm (therefore shoulder beam behaves a rigid body), L_2=50 µm and the dome angle $\alpha = 15^{\circ}$ are considered for a preferable design response. The corresponding values of polyslicon E = 165 GPa.

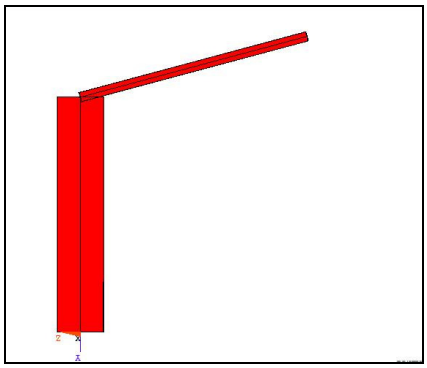

Figure3.7: Half of the candidate mechanism model in ANSYS

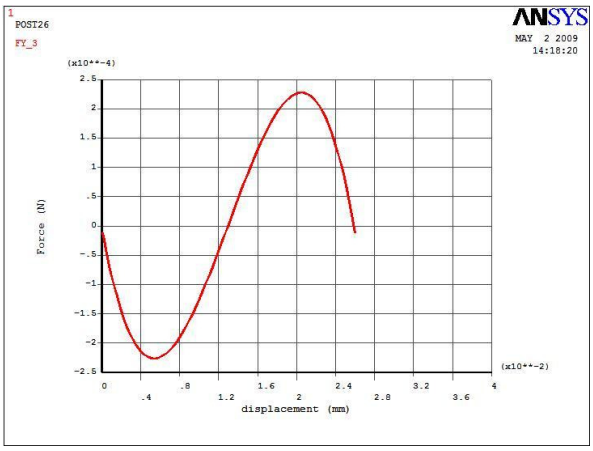

Figure 3.8: Force-deflection curve of the candidate mechanism

4. BRIEF INTRODUCTION TO ANALYTICAL DYNAMICS

Dynamical modelling of a mechanical system is one of the most important tasks an engineer should implement. There are some basic and powerful technics to obtain a dynamic model. Most fundemental and well-known technic is based on the Newton's laws of motion. The equations of motions are expressed in terms of physical coordinates and forces and both quantities are represented by vectors. For this reason, Newtonian mechanics is often refered to as vector mechanics. Newtonian mechanics requires a free body diagram for each of the masses in the system and includes reaction forces and ineracting forces. Application of newtonian mechanics for comlex systems is extremely challenging and almost impossible and useless to prepare a general purpose computer programs.

A different approach referred to as analytical dynamics are based on the total kinetic and potential energy of the system and much more powerful than Newtonian mechanics. Equations of motions in this approach are formulated in terms of two scalar functions and an initesimal expression, the virtual work performed by the nonconservative forces [19]. Generalized coordinates and generealized forces with any special system of coordinates are used to prepare the model of the system. In this approach a powerful technic called Lagrange equations are used to obtain dynamic model of systems. This method is also called Lagrangian dynamics. To obtain a dynamic model of a system, one approach is to represent the dependent coordinates in terms of independent coordinates. This enables to model the system with minimum system of equations that is as the same number as the system degrees of freedom. The second and much general approach is to use generalized coordinates to represent the position and orientation of each partical of the system. In this approach, dynamic model is obtained in terms of generalized forces and coordinates[19]. And system of equations are solved simultaneously with the constraint equations which are nonlinear system of equations. The number of equations is the same as the generalized coordinates used to model the system. This kind of formulation leads to the preparation of a general purpose computer program such as ADAMS.

Since a computer algorithm does not recognize which coordinates are independant or not, system is represented by dynamic equations written in terms of generalized coordinates and the relation between each part is computed with constraint equations.

4.1 Generalized Coordinates

In formulating dynamical system, one of the possibilities is to use the physical coordinates which may not always be independent. As an example, consider a dummbell in figure 5.1 consisting of two masses connected by a massless rigid bar of length L. Assuming a planar motion, we can define the motion by the porsition vector $\mathbf{r}_1$ and $\mathbf{r}_2$. These vectors involve for coordinates x_1, x_2, y_1 and y_2.

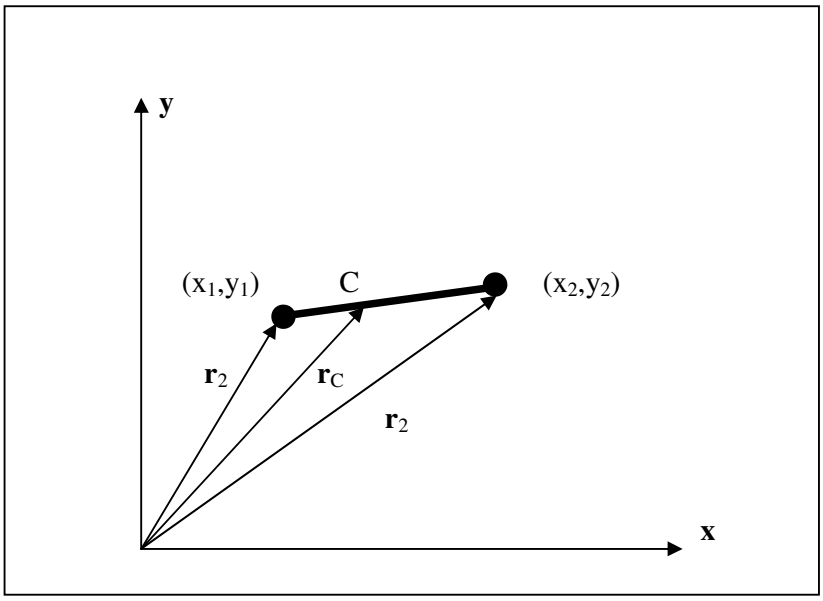

Figure 4.1: Coordinate of a particle

But these four coordinates are related by the equation

$$(x_2 - x_1)^2 + (y_2 - y_1)^2 = L^2 \qquad \textbf{(4.1)}$$

which represents a constraint equation. Since each term in this equation is represented in terms of the remaining three, system degrees of freedom is equal to three which means only three coordinates are independent. If this four coordinates are chosen, the problem is formulated in terms of these coordinates and the constrained equation. A better choise of coordinates eliminates this constraint equation.

In planar motion only three coordinates, which are x_C, y_C and θ, are necessary to define the position of the particle. Here x_C and y_C are the componets of $\mathbf{r}_C$ and θ represents the orientaiton of the particle with respect to global coordinate system.

These random chosen coordinates are called *generalized coordinates.* Any set of generalized coordinates can be used to formulate the equations of motion. In many multibody computer programs generalized coordinates are used for the sake of generality. Formulation of the equations of motion is prepared for each part using related generalized coordinates and constraint equations between the components are solved simultaneously to include the kinematic relations between each part.

4.2 Priciple of Virtual Work

Principles of virtual work is a tool for transition form Newtonian mechanics to Lagrangian mechanics. It is based on variational calculus and the first variation. Definition of virtual displacements and generalized forces is important in the application of the principle of virtual work.

4.2.1 Virtual displacements

Virtual displacement is defined to be an infinitesimal change of the position of a point on the body. Position vector of an arbitrary point is given by the equation :

$$\mathbf{r}_P^i = \mathbf{R}^i + \mathbf{A}^i \cdot \bar{\mathbf{u}}_P^i \qquad \textbf{(4.2)}$$

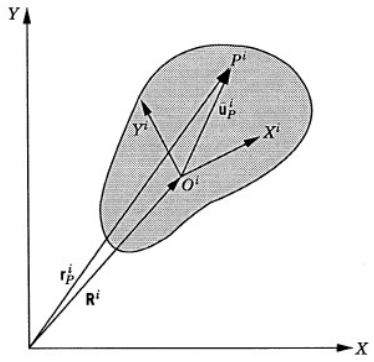

Figure 4.2: Position representation of a mass

$\mathbf{R}^{i}$ is the position vector of the reference point, $\bar{\mathbf{u}}_{P}^{i}$ is the position vector of point P^{i} with respect to the reference point O^{i} and $\mathbf{A}^{i}$ is the transformation matrix given by

$$\mathbf{A}^{i} = \begin{bmatrix} \cos\theta^{i} & -\sin\theta^{i} \\ \sin\theta^{i} & \cos\theta^{i} \end{bmatrix} \tag{4.3}$$

In equation 5.3, θ is the orientation of the body. Virtual change in the position vector of point P^{i} is ddenoted as $\delta\mathbf{r}_{P}^{i}$ and is given by the equation

$$\delta\mathbf{r}_{P}^{i} = \delta\mathbf{R}^{i} + \delta(\mathbf{A}^{i} \cdot \bar{\mathbf{u}}_{P}^{i}) \tag{4.4}$$

and this equation can be written as

$$\delta\mathbf{r}_{P}^{i} = \delta\mathbf{R}^{i} + \mathbf{A}_{\theta}^{i} \cdot \bar{\mathbf{u}}_{P}^{i} \cdot \delta\theta^{i} \tag{4.5}$$

where

$$\mathbf{A}_{\theta}^{i} = \frac{\partial\mathbf{A}^{i}}{\partial\theta^{i}} = \begin{bmatrix} -\sin\theta^{i} & -\cos\theta^{i} \\ \cos\theta^{i} & -\sin\theta^{i} \end{bmatrix} \tag{4.6}$$

4.2.2 Virtual work and generalized forces

Virtual work of a force vector is defined to be the dot product of the force vector and the vector of the virtual change of the position vector of the point of application of the force. Both vectors must be defined in the same coordinate system. Virtual work of a moment is also defined to be the product of the moment and the angular orientation of the body [19].

Figure shows the moment M^{i} and the force $\boldsymbol{F}^{i}$ acting upon the body. And the point of application is denoted as P^{i}. Virtual work of these forces is given by

$$\delta W^{i} = \boldsymbol{F}^{i^{T}} \delta\boldsymbol{r}_{P}^{i} + M^{i} \cdot \delta\theta \tag{4.7}$$

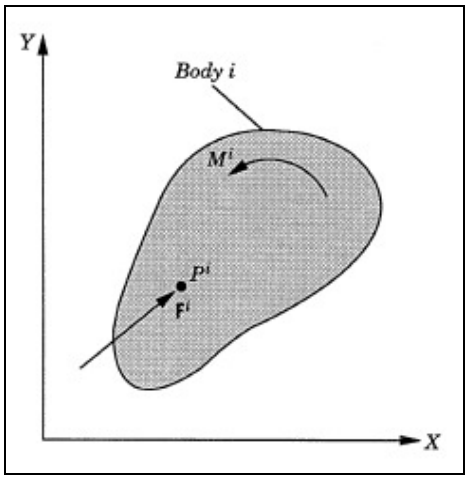

Figure 4.3: Forces acting on a particle

The position vector of an arbitrary point on a rigid body can be expressed in terms of the position vector of the reference point and the angular orientation of the body. This position vector is given as;

$$\mathbf{r}_P^i = \mathbf{R}^i + \mathbf{A}^i \cdot \bar{\mathbf{u}}_P^i \tag{4.8}$$

Using the virtual displacements of the position vector and the forces acting on this point of application, virtual work of these forces can be written as

$$\delta W^i = \boldsymbol{F}^{iT}(\delta \mathbf{R}^i + \mathbf{A}_\theta^i \cdot \bar{\mathbf{u}}_P^i \cdot \delta\theta^i) + M^i \cdot \delta\theta \tag{4.9}$$

$$\delta W^i = \boldsymbol{F}^{iT}\delta \mathbf{R}^i + (\boldsymbol{F}^{iT}\mathbf{A}_\theta^i \cdot \bar{\mathbf{u}}_P^i + M^i)\delta\theta^i \tag{4.10}$$

In this equation, $\boldsymbol{F}^i$ is the *generalized force* associated with the coordinates of reference point and $(\boldsymbol{F}^{iT}\mathbf{A}_\theta^i \bar{\mathbf{u}}_P^i + M^i)$ is the *generalized force* associated with the rotation of the body. And the statement of the principle of virtual work is that the work performed by the applied forces through infinitesimal virtual displacement is equal to zero if the system is in static equilibrium.

4.3 d'Alembert Principle

The priciple of virtual work is concerned with the static equilibrium of the systems. However, the virtual work priciple can be extended to dynamics in which form it is

known as d'Alembert's principle. This principle includes the work performed by the inertia forces of the parts. And for a rigid body, equations of motions are given as;

$$\mathbf{F}^i - m^i \cdot \mathbf{a}^i = 0$$

(4.11)

$$M^i - J^i \cdot \ddot{\theta}^i = 0 \qquad \textbf{(4.12)}$$

So the virtual work performed by these forces is given as;

$$(\mathbf{F}^i - m^i \cdot \mathbf{a}^i)^T \delta \boldsymbol{R} + (M^i - J^i \cdot \ddot{\theta}^i)\delta\theta = 0 \qquad \textbf{(4.13)}$$

This principle can be used to obtain the equations of motions of multibody systems. In order to obtain the equation, dependent coordinates are represented by the independent coordinates and the work performed by each force are computed. Knowing that $\delta \boldsymbol{R}$ and $\delta\theta$ is equal to zero, coefficients of this virtual statements are also equal to zero and the equations obtained from this calculation gives the equation of motions of the system.

4.4 Lagrange's Equations

To obtain the dynamic equations of motion of a system, a powerful and easy to implement technic is derived by Lagrange. The prrincipal of virtual work allows us to formulate the dynamic equations using any set of generalized coordinates.

According to Lagrange's formulation, generalized inertia forces of rigid bodies can be given as;

$$\mathbf{Q}_\mathrm{i} = \frac{\mathrm{d}}{\mathrm{dt}}\left(\frac{\partial \mathrm{T}}{\partial \dot{\mathbf{q}}_\mathrm{i}}\right)^\mathrm{T} - \left(\frac{\partial \mathrm{T}}{\partial \mathbf{q}_\mathrm{i}}\right)^\mathrm{T} \qquad \textbf{(4.14)}$$

T is the system total kinetic energy, obtained using independent generalized coordinates. **q** is the vector generalized coordinates associated with body i.

Using the principle of virtual work and d'Alembert principle, system equations of motion can be given as

$$\frac{d}{dt}\left(\frac{\partial T}{\partial \dot{q}_j}\right)-\left(\frac{\partial T}{\partial q_j}\right)=Q_j \qquad j=1,2,3,....,n \tag{4.15}$$

Here $q_j, j=1,2,...,n$ are the independent coordinates of the system degrees of freedom and Q_j is the generalized applied force associated with the independent coordinate q_j. This equation is called Lagrange's equations of motion.

4.5 Hamiltonian Formulation

The forces acting on a mechanical system can be classified as conservative and nonconservative forces. Vector of generalized forces acting on a multibody system can be written as

$$\mathbf{Q}_e=\mathbf{Q}_{nc}+\mathbf{Q}_{co} \tag{4.16}$$

$\mathbf{Q}_{co}$ and $\mathbf{Q}_{nc}$ are the vector of conservative and nonconservative forces. And conservative forces can be derived from a potential function V as

$$\mathbf{Q}_{co}=-\left(\frac{\partial V}{\partial \mathbf{q}}\right) \tag{4.17}$$

$\mathbf{q}=[q_1....q_n]^T$ is the vector of generalized coordinates. This equation gives

$$\mathbf{Q}_e=-\left(\frac{\partial V}{\partial \mathbf{q}}\right)+\mathbf{Q}_{nc} \tag{4.18}$$

and

$$\mathbf{Q}_e=\frac{d}{dt}\left(\frac{\partial T}{\partial \dot{\mathbf{q}}}\right)^T-\left(\frac{\partial T}{\partial \mathbf{q}}\right)^T \tag{4.19}$$

Knowing that the potential function V does not depend on the generalized velocities, system equations of motion can be written as

$$\frac{d}{dt}\left(\frac{\partial(T-V)}{\partial \dot{\mathbf{q}}}\right)^{T}-\left(\frac{\partial(T-V)}{\partial \mathbf{q}}\right)^{T}=\mathbf{Q}_{nc} \qquad \textbf{(4.20)}$$

Here L=T-V is called the Lagrangian.

4.6 Lagrange Multipliers

In a multibody system, if the dependent coordinates are defined in terms of independent ones and write the system of equations in terms of independent coordinates, joint reaction forces are automatically eliminated from the equation. A second approach is to include the work done by reaction forces in the equations of motion. So, the generalized forces induced by reaction forces of the system have to be defined. This approach is useful and widely used in computational dynamics since the constraint forces are defined by a set of lagrange multipliers and this enables us to write a general purpose computer algorithm regardless of the structure of the system. Consider a planar system that consists of two rigid bodies. These two bodies are connected at point P by a revolute joint.

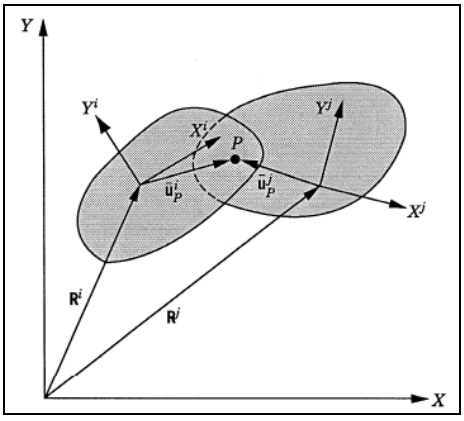

Figure 4.4: Constraint between two bodies

Constraint equations for a planar revolute joint is given as

$$\mathbf{R}_i+\mathbf{A}_i.\bar{\mathbf{u}}_P^{\,i}-\mathbf{R}_j+\mathbf{A}_j.\bar{\mathbf{u}}_P^{\,j}=0 \qquad \textbf{(4.21)}$$

$$\theta_i - \theta_j = 0 \tag{4.22}$$

Here $\mathbf{R}_i$ and $\mathbf{R}_j$ are the global position vectors of the origins of the coordinate systems of bodies i and j. $\mathbf{A}_i$ and $\mathbf{A}_j$ are the transformation matrices of the coordinate systems of body i and body j to the global coordinate system. $\bar{\mathbf{u}}_P^i$ and $\bar{\mathbf{u}}_P^j$ are the local position vectors of point P with respect to the reference points of body i and j. θ_i and θ_j are the angular orientations of body i and body j. Constraint equations can be wrritten in a matrix form as

$$C = \begin{bmatrix} \mathbf{R}_i + \mathbf{A}_i \cdot \bar{\mathbf{u}}_P^i - \mathbf{R}_j + \mathbf{A}_j . \bar{\mathbf{u}}_P^j \\ \theta_i - \theta_j \end{bmatrix} = 0 \tag{4.23}$$

Constraint jacobian matrix of these constraint equations is given in a partitioned form as

$$\mathbf{C}_{\mathbf{q}^i} = \begin{bmatrix} I & \mathbf{A}_\theta^i . \bar{\mathbf{u}}_P^i \\ 0 & 1 \end{bmatrix} \tag{4.24}$$

$$\mathbf{C}_{\mathbf{q}^j} = \begin{bmatrix} I & \mathbf{A}_\theta^j . \bar{\mathbf{u}}_P^j \\ 0 & 1 \end{bmatrix} \tag{4.25}$$

Here $\mathbf{A}_\theta^i$ and $\mathbf{A}_\theta^j$ are the partial derivatives of the transformation matrices $\mathbf{A}^i$ and $\mathbf{A}^j$ with respect to θ_i and θ_j.

4.6.1 Equipollent system of forces

Forces acting on a random point of a body can be replaced by the forces acting on the coordinate systems of bodies. This reperesentation does not change the dynamics of the system and the work done by two different type of forces is the same. This system of forces is called equipollent system of forces. This representation can be considered as the generalization of the forces acting on the body.

If we let $\boldsymbol{\lambda}$ be the vector

$$\boldsymbol{\lambda} = \begin{bmatrix} \mathbf{F} \\ \mathrm{M} \end{bmatrix} \tag{4.26}$$

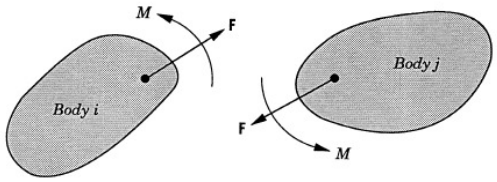

Figure 4.5: Constraint forces

The reaction forces acting on body i and j which are equal in magnitude and opposite in direction can be expressed in a vector form as

$$\mathbf{F}^{\mathrm{i}} = -\boldsymbol{\lambda} = \begin{bmatrix} \mathbf{F} \\ \mathrm{M} \end{bmatrix} \quad \text{and} \quad \mathbf{F}^{\mathrm{j}} = \boldsymbol{\lambda} = -\begin{bmatrix} \mathbf{F} \\ \mathrm{M} \end{bmatrix} \tag{4.27}$$

Equipollent system of forces defined at the origins of the coordinate systems of two bodies is given as

$$\mathbf{Q}_{\mathrm{c}}^{\mathrm{i}} = \begin{bmatrix} \mathbf{F} \\ \mathrm{M} + \bar{\mathbf{u}}_{\mathrm{P}}^{\mathrm{i}\,\mathrm{T}}\, \mathbf{A}_{\theta}^{\mathrm{i}\,\mathrm{T}} \mathbf{F} \end{bmatrix} \tag{4.28}$$

$$\mathbf{Q}_{\mathrm{c}}^{\mathrm{j}} = \begin{bmatrix} \mathbf{F} \\ \mathrm{M} + \bar{\mathbf{u}}_{\mathrm{P}}^{\mathrm{j}\,\mathrm{T}}\, \mathbf{A}_{\theta}^{\mathrm{j}\,\mathrm{T}} \mathbf{F} \end{bmatrix} \tag{4.29}$$

This equation is the same as generalized forces explained in the preceeding sections. In this case, these equations are called generalized reaction forces.

4.6.2 Definition of lagrange multipliers

Generalized reaction forces can be written as

$$\mathbf{Q}_{\mathrm{c}}^{\mathrm{i}} = \begin{bmatrix} \mathbf{I} & 0 \\ \bar{\mathbf{u}}_{\mathrm{P}}^{\mathrm{i}\,\mathrm{T}} & \mathbf{A}_{\theta}^{\mathrm{i}\,\mathrm{T}} 1 \end{bmatrix} \begin{bmatrix} \mathbf{F} \\ \mathrm{M} \end{bmatrix} \tag{4.30}$$

$$\mathbf{Q}_{\mathrm{c}}^{\mathrm{j}} = \begin{bmatrix} \mathbf{I} & 0 \\ \bar{\mathbf{u}}_{\mathrm{P}}^{\mathrm{j}\,\mathrm{T}} & \mathbf{A}_{\theta}^{\mathrm{j}\,\mathrm{T}} 1 \end{bmatrix} \begin{bmatrix} \mathbf{F} \\ \mathrm{M} \end{bmatrix} \tag{4.31}$$

If we compare the square matrices in these equations, we obtain the equations below

$$\mathbf{Q}_c^i = -\mathbf{C}_{\mathbf{q}^i}^T \boldsymbol{\lambda} \qquad \textbf{(4.32)}$$

$$\mathbf{Q}_c^j = -\mathbf{C}_{\mathbf{q}^j}^T \boldsymbol{\lambda} \qquad \textbf{(4.33)}$$

Here $\boldsymbol{\lambda}$ is called the Lagrange multiplier.

4.7 Generalized System of Equations

From the equations and definitions below, a generalized equation that can be used to formulate the dynamic equations of motion of any mechanical system can be obtained. This equation can be written as;

$$\frac{d}{dt}\left(\frac{\partial L}{\partial \dot{\mathbf{q}}}\right)^T - \left(\frac{\partial L}{\partial \mathbf{q}}\right)^T + \boldsymbol{\lambda}\frac{\partial \mathbf{Q}}{\partial \mathbf{q}} - \mathbf{Q}_{nc} = 0 \qquad \textbf{(4.34)}$$

Another representation of this equation can be written as

$$\frac{d}{dt}\left(\frac{\partial L}{\partial \dot{\mathrm{q}}_\mathrm{i}}\right) - \left(\frac{\partial L}{\partial \mathrm{q}_\mathrm{i}}\right) + \sum_{j=1}^{m} \lambda_\mathrm{j} \cdot \frac{\partial \mathrm{Q}_\mathrm{j}}{\partial \mathrm{q}_\mathrm{i}} - \sum_{k=1}^{na} F_k \cdot \frac{\partial r_k}{\partial q_i} = 0 \qquad \mathrm{i} = 1,2,.....\mathrm{n} \qquad \textbf{(4.35)}$$

L = T – V = Lagrangian

Q = Constraint equations

r = Application point of force

q = Generalized coordinates

F = Externally applied force

λ = Lagrange multipliers

Using this equation, a set of second order differential equations is obtained. Solving these differential equations with the nonlinear algebric constraint equations, dynamic behaviour of a mechanical system is simualted.

Constraint equations for different types of joint constraints are available in literature, and one can use these equations and extend it to the tree dimensional case in order to obtain the dynamic equations of motion of a system in space.

5. DYNAMICAL MODELING OF THE ROTATIONAL DWELL MECHANISM

It is one of the most important tasks to simulate the dynamic behavior of a mechanism designed. Dynamical simulation enables engineers to be able to see how a mechanical system reacts under the forces and moments acting on the mechanism. Another thing that dynamical simulation offers is to compute the reaction forces at each joint which may use as the next step to compute the mechanical behavior of the system such as stress calculation, deformation on each component. So a design optimization procedure may be employed to have an optimized component. And some of the mechanical parts such as connecting rods and pistons run in operation conditions where very high speeds exist. In such machines as internal combustion engines it becomes very important to consider the forces induced by inertia affects of components. Actually in internal combustions engines which run according to otto cycle forces acting on the parts of the engine reach to their maximum value at the maximum operating speed. Thus, the stress distribution and fatigue life of the components are calculated according to maximum forces which occur at maximum speed.

Dynamical simulation combined with finite element analysis enables computation of the behavior of components simultaneously considering the elastic behavior of the system.

5.1 Adams Model of Rotational Dwell Mechanism

Mechanism is composed of four elements; two is modeled as rigid arms the other two are modeled as spring elements. In this package it is possible to define the spring constant as a constant, matematical model or a tablo which is interpolated. In this application, the table is chosen to interpolate as spline. For this purpose, the points load-deflection curve which is obtained in the non-linear solution of FEM

program is put in the spring coefficient table. So, the spring simulated the same model of flexible arm beam which we obtained in FEM anaylsis. To view the results, sensor elements are used on the joints between the follower and the ground and between the crank and the ground.

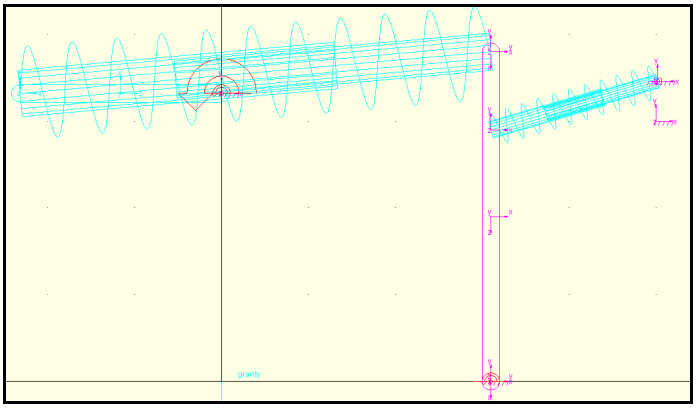

Figure 5.1: Two dimensional view of the ADAMS model

The simulation is conducted as the crank moves with a constant speed of 1.3 rad/sn for 5 seconds. At the results of the simulation, until the crank angle becomes 155 degree the short arm beam is compressed with the varying load which is under the critical buckling load so that the beam stays stable at the initial condition. After buckling, the deformation occurs till the follower snaps to the other stable condition. When the joints at the each end of the flexible beam become alligned horizontally, the follower snaps to the second stable position faster, because the beam forces act on the same side of the follower. As the crank angle is between 180 and 247, follower stays at the second stable condition. When the crank angle becomes 247, tensile force acts on the long flexible beam because of the geometrical constraints. This movement forces the short flexible beam to move in the direction of initial condition. So, buckling occurs secondly in the opposite direction. During the deflection of the short beam, the long beam stays straight as a rigid element so that the speed of the follower and the deformation of the beam become dependent on the speed of the crank angle. As the forces of two beams are in opposite direction while the snap occurs this second snap becomes slower than the first snap of the beam.

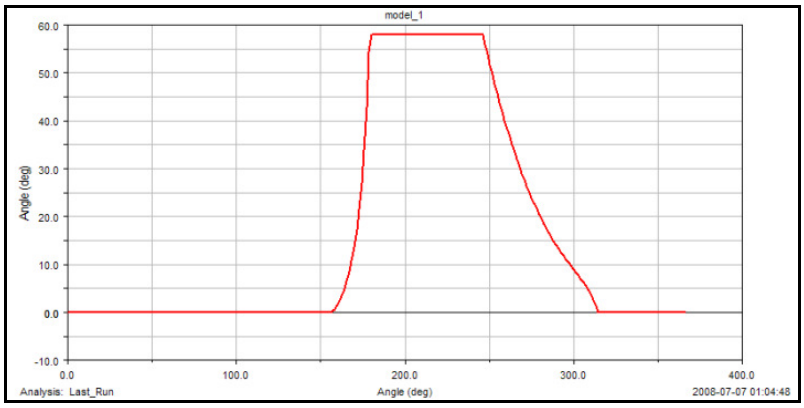

Figure 5.2: The change of follower angle during 360º rotation of crank arm

As we eliminate the moment of inertia and the mass terms of the follower and the crank in the simulation, we obtain the statical response of the mechanism as in the figure 5.3.

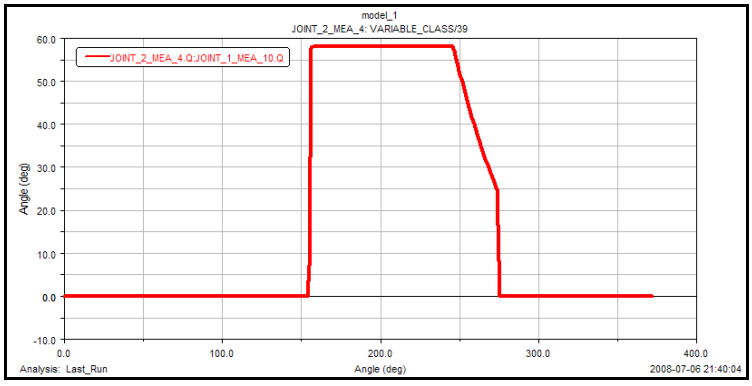

Figure 5.3: Quasi-statical change of follower angle to crank angle

6. MECHANISM MODELED BY SIMULINK

6.1 Loop Closure Equations

There are two closed loops in the mechanism. The crank, follower and the first flexible beams are the members of the first loop. The second one is between the follower and the second flexible beam.

$$\begin{aligned} &R_2 \cdot \cos(\theta_2) + R_1 \cdot \cos(\theta_1) + R_4 \cdot \cos(\theta_4) = R_3 \cdot \cos(\theta_3) \\ &- R_2 \cdot \sin(\theta_2) - R_1 \cdot \sin(\theta_1) + R_4 \cdot \sin(\theta_4) = R_3 \cdot \sin(\theta_3) \end{aligned} \quad \textbf{(6.1)}$$

$$\begin{aligned} &R_6 \cdot \sin(\theta_6) - R_4 \cdot \sin(\theta_4) = R_5 \cdot \sin(\theta_5) \\ &R_6 \cdot \cos(\theta_6) - R_4 \cdot \cos(\theta_4) = R_5 \cdot \cos(\theta_5) \end{aligned} \quad \textbf{(6.2)}$$

6.2 Force Deflection Equation

The Deflection-Froce curve has been obtained by geometrically non-linear statical analysis. Here to obtain a result closer to theoretical solution, the curveture after the buckling fitted by a 3rd order polinomial. The linear elongation equation is used in the prebuckling period solution.

$$F(\Delta R_3) = \frac{Sign(L_C - \Delta R_3) + 1}{2} \cdot \frac{E \cdot A \cdot \Delta R_3}{L} + \frac{Sign(\Delta R_3 - L_C) + 1}{2} \cdot a \cdot \Delta R_3^{\,3} + b \cdot \Delta R_3^{\,2} + c \cdot \Delta R_3 + d \quad \textbf{(6.3)}$$

$$F(\Delta R_5) = \frac{Sign(L_C - \Delta R_5) + 1}{2} \cdot \frac{E \cdot A \cdot \Delta R_5}{L} + \frac{Sign(\Delta R_5 - L_C) + 1}{2} \cdot a \cdot \Delta R_5^{\,3} + b \cdot \Delta R_5^{\,2} + c \cdot \Delta R_5 + d \quad \textbf{(6.4)}$$

6.3 Dynamic Equation

$$I \cdot \ddot{\theta}_4 = R_{4a} \cdot F_{R3} \cdot \cos(\theta_3 - (pi/2 - \theta_4)) - R_{4b} \cdot F_{R5} . \cos(\theta_5 + (pi/2 - \theta_4)) \quad \textbf{(6.5)}$$

θ_4 is obtained by integrating $\ddot{\theta}_4$ from the above equation. This signal is supplied to the kinematik loop closure equations to be used in the next step of the numerical solution.

6.4 Simulation Results

The simulation is solved by the fourth order Runge-Kutta method. Ignoring the dynamics of the DC motor, the speed of the motor is given as a constant variable which is the input of the dynamic system model. The equations given in the previous sections are solved and the angular displacement of follower is obtained due to the displacement of the crank. The density of the material is decreased here to see the inertial effects.

The results obtained in figure 6.2 are the same as the ones obtained by ADAMS. Only, the return time is shorter here because of the decreased inertia.

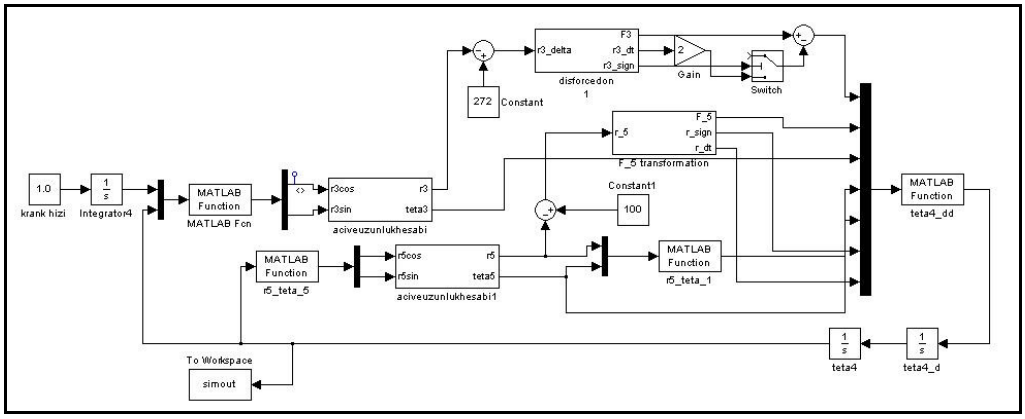

Figure 6.1: Simulink model of the rotational exact dwell mechanism

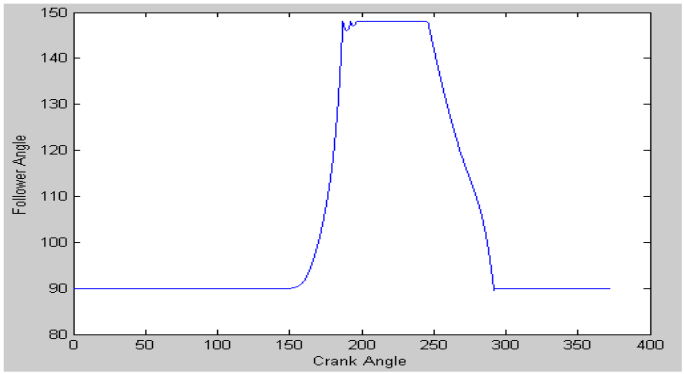

Figure 6.2: Dynamic response of follower angle to the crank angle change

7. PRODUCTION OF ROTATIONAL DWELL MECHANISM IN MACRO LEVEL

7.1 Making of the Dwell Mechanism In the Scope of the Motion Parameters

Mechanism is build on a ractangular wooden table. The making of the mechanism is started from the rigid follower arm. Firstly, the follower arm is assembled on the board for the easiness of the complation of the mechanism. The follower has three joints:one is attached from the horizontal revolution center to the board and the encoder, one is attached to the short beam and the the other end of the arm is attached to the long beam. The distance between the revolute joint and the one linked to the short beam is close to the length of the short beam. By this choise, the snap angle range is large enough to have a good response. During the buckling, the minimum distance between the ends of the short beam is chosen to be short that the force that cause the snap of the beam is higher. So, the follower reaches quick enough to view to the second stable condition.

Figure 7.1: Top view of the dwell mechanism board

The joints on the each end of the flexible arm beams have quite low friction that the tortional moment is does not deform the beams significantly.

The objective of the second stage of mechanism making is to obtain the enough force magnitude. The kinetic energy is transfered to the short arm beam. The magnitudes that affect the applied force to the follower are the thickness width and the lenght of the beam and the distance between the beam-follower arm joint and the follower arm-ground joint. The joint of long beam has longer distance to the center of revolution. So that the short beam geometric parameters have less sensitivity to the changes and it is easier to make a modification due to the dwell parameters. Before making of mechanism no kinematic syntesis has been done, the beam parameters has been chosen approximately before the position of the motor. After a few iterative steps, optimum position of the crank revolution center and the crank length is defined.

7.2 Flexible Arm Beams

As the flexible arm beams stripe springs are chosen. These are produced as plates made of steel and sliced as plates gyotine scissors. The length-thickness ratios are chosen that bending does not cause significant plastic deformation.

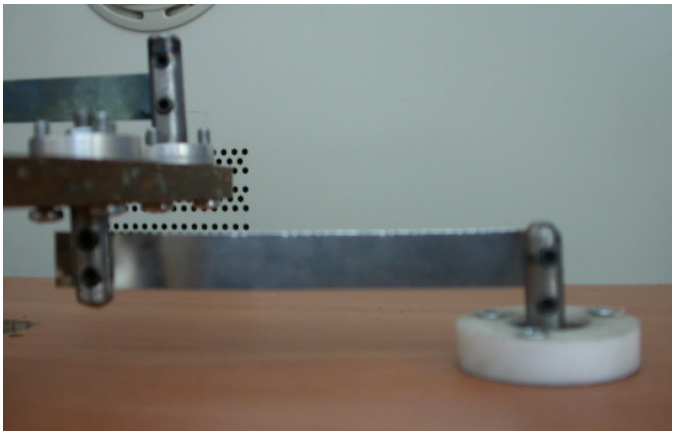

Figure 7.2: Short flexible beam and the joints

7.3 Joints

The flexible arm beams are connected with pin-pin joint elements. This connection is composed of 5 cm lenght shafts that revolute in ball bearings. The shafts are cut from the mid points to attach the beam elements with the compressive force of bolts as in the figure. This type of connection made it possible to change the beam members in case of deformation or unwanted motion characteristics.

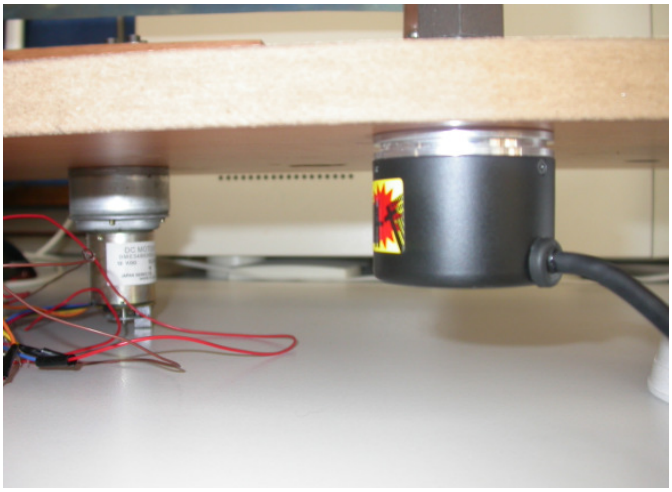

Figure 7.3: Encoder and DC motor

The encoders and the DC motor has been assembled to the table from the other face. The shaft of the DC motor has been lenghtened for the other encoder to obtain the crank angle with a high precision.

7.4 Results of Quasi-Statical Measurement

The measurements are done quasi-statically The snap though motion and the dwell period is obtained as expected varifing the simulation results with a proposed difference.

While the crank arm moves between 0 and 115, the follower stays at the first stable condition. Till 150 degree, short beam continous to deform. This is the unexpected response due to the simulation results because of the prestresses on the short beam. After the crank passes 150 degree the follower snaps to the second stable position.

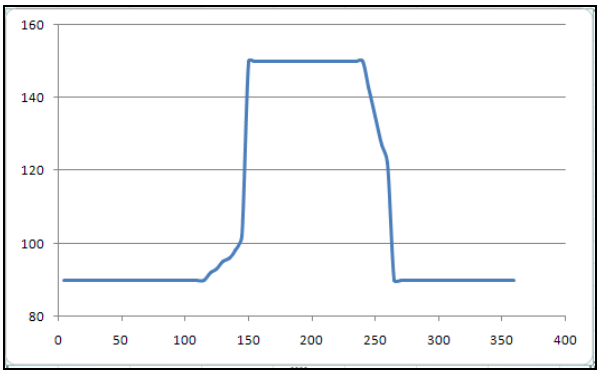

Figure 7.4: The change of the measured follower angle due to the crank rotation

8. CONCLUSION AND RECOMMENDATIONS

The major purpose of this research was to present the methodology of compliant mechanism design with examples of compliant mechanisms and to validate a novel design of a rotational compliant exact double dwell five bar mechanism. The mechanism was build successfully so that the sheet springs did not have plastic deformation and give a good response to observe the charactheristics of the motions. The dynamical simulations are conducted in two different methods. The one done by the package program called ADAMS gave more precise solutions as the unknown parameters are solved by the solution of a set of non-linear equations shown in the section 4. The Simulink model containing the non-linear equations of dynamics are directly iterated by a very small sample size which gave solutions similar to the ones obtained by ADAMS considering the dwell parameters. This solutions can be observed for the dwell time, rise time and return time characteristics. Both of the stable positions were observed as the dwell occurs in each position in both simulation results as expected. The statical results are validated with the datas observed on the mechanism.

REFERENCES

[1] **Howell, L.L.**, 2001. *Compliant Mechanisms*, 1st edition John Wiley & Sons, Inc., New York

[2] **Euler, L.,** (1744). *Methodus Inveniendi Lineas Curvas. Lausanne and Geneva*, English Translation by Oldfather, W.A., Ellis, C.A. and Brown, D.M.

[3] **Bisshopp, K.E., Drucker, D.C.,** (1945). Large deflections of cantilever beams. *Quarterly of Applied Mathematics,* **3(3)**, 272-275.

[4] **Frisch Fay, R.** (1962). *Flexible Bars*, ButterWorths, London.

[5] **Shoup, T.E., McLarnan, C.W.** (1971a). On the use of the undulating Elastica for the analysis of flexible link mechanisms. *Journal of Engineering for the Industry, Transactions of the ASME,* February 263-267.

[6] **Shoup, T.E., McLarnan, C.W.** (1971b). On the use of a doubly clamped flexible strip as a nonlinear spring. *Journal of Engineering for the Industry. Transactions of the ASME,* June 559-560.

[7] **Shoup, T.E.** (1969). An analytical investigation of the large deflections of flexible beam springs. *Ph.D. Dissertation*, The Ohio State University, Columbus, Ohio.

[8] **Mattiasson, K.** (1981). Numerical results from large deflection beam and frame problems analyzed by means of elliptic integrals. *International Journal of Numerical Methods in Engineering, Short Communications*, **17(1),** 145-153.

[9] **Gorski, W.** (1976). A review of literature and a bibliography on finite elastic deflections of bars. *The Institution of Engineers, Australia Civil Engineering Transactions,*74-85.

[10] **Navaee, S., Elling, R.E.** (1992). Equilibrium configurations of cantilever beams subjected to inclined end loads. *ASME Journal of Applied Mechanics,* **59**, 572-579.

[11] **Abe, T., Messner, W.C., and Reed, M.L.,** 1995. Effective methods to prevent stiction during post-release-etch processing, *Proceedings of IEEE Micro Electro Mechanical Systems 1995*, 95CH35754, 94-99.

[12] **Gomm, T., Howell, L. L., and Selfridge, R. H.**, 1997: In-Plane Linear Displacement Bistable Micro Relay, *Journal of Micromechanisms & Microeng*., **12**, 257-264

[13] **Sönmez, Ü.,** 2006. A compliant bistable mechanism design incorporating elastica buckling beam theory and pseudo rigid body model, *Journal of Mechanical Design*, **130**, 2-13.

[14] **Sönmez, Ü.,** 2000. Compliant mechanism design and synthesis using buckling and snap-through buckling of flexible members. *Ph.D. Thesis*, The Pennsylvania State University, State College, PA.

[15] **Berkof, M.P.,** (1996). Design methodology for a long dwell finite dell linkage. *Master Thesis*, The Pennsylvania State University.

[16] **Badre-Alam, A., Streit, D.A.**, (1994). Long-dwell and finite-dwell linkages. *ASME Mechanism Synthesis and Analysis Conference* pp. 479-485.

[17] **Norton, R.L.** (1999). *An Introduction to the Synthesis and Analysis of Mechanisms and Machines*, 2nd edition, McGraw-Hill.

[18] **Byrd, P.F., Friedman**, **M.D**. (1954). *Handbook of Elliptic Integrals for Engineers and Physicists,* Springer-Verlag, Berlin

[19] **Shabana, A.A.,** 2001. *Computational Dynamics*, John Wiley & Sons, Chicago.

CURRICULUM VITA

Candidate's full name:	Barboros BENSOY
Place and date of birth:	11.04.1984
Permanent Address:	Uzunçayır Yolu Sok.,No:38, D:10, Merdivenköy, GÖZTEPE/KADIKÖY
Universities and Colleges attended:	ITU Mechanical Engineering